The International Journal of Advanced Manufacturing Technology (2024) 134:453–475
https://doi.org/10.1007/s00170-024-14144-z

ORIGINAL ARTICLE

Wire arc additive manufacturing of a high-strength low-alloy steel part: environmental impacts, costs, and mechanical properties

Samruddha Kokare[1,3] · Jiajia Shen[2] · Pedro P. Fonseca[1] · João G. Lopes[1] · Carla M. Machado[1,3] · Telmo G. Santos[1,3] · João P. Oliveira[2] · Radu Godina[1,3]

Received: 14 March 2024 / Accepted: 12 July 2024 / Published online: 22 July 2024

Abstract

Additive manufacturing (AM) technologies have demonstrated a promising material efficiency potential in comparison to traditional material removal processes. A new directed energy deposition (DED) category AM process called wire arc additive manufacturing (WAAM) is evolving due to its benefits which include faster build rates, capacity to build large volumes, and inexpensive feedstock materials and machine tools compared to more technologically mature powder-based AM technologies. However, WAAM products present challenges like poor surface finish and lower dimensional accuracy compared to powder-based processes or machined parts, prevalence of thermal distortions, residual stresses, and defects like porosity, cracks, and humping, often requiring post-processing operations like finish machining and heat treatment. These post-processing operations add to the production cost and environmental footprint of WAAM-built parts. Therefore, considering the opportunities and challenges presented by WAAM, this paper analyses the environmental impact, production costs, and mechanical properties of WAAM parts and compares them with those achieved by laser powder bed fusion (LPBF) and traditional computer numerical control (CNC) milling. A high-strength low-alloy steel (ER70S) mechanical part with medium complexity was fabricated using WAAM. Based on the data collected during this experiment, environmental impact and cost models were built using life cycle assessment and life cycle costing methodologies. WAAM was observed to be the most environmentally friendly option due to its superior material efficacy than CNC milling and has a better energy efficiency than LPBF. Also, WAAM was the most cost-friendly option when adopted in batch production for batch sizes above 3. The environmental and cost potential of WAAM is amplified when used for manufacturing large products, resulting in significant material, emission, and cost savings. The fabricated WAAM part demonstrated good mechanical properties comparable to that of cast/forged material. The methodology and experimental data presented in this study can be used to calculate environmental impacts and costs for other products and can be helpful to manufacturers in selecting the most ecofriendly and cost-efficient manufacturing process.

Keywords Life cycle assessment · Life cycle costing · Mechanical characterization · Wire arc additive manufacturing · CNC machining · Laser powder bed fusion

✉ Samruddha Kokare
s.kokare@campus.fct.unl.pt

[1] UNIDEMI, Department of Mechanical and Industrial Engineering, NOVA School of Science and Technology, Universidade NOVA de Lisboa, 2829-516 Caparica, Portugal

[2] CENIMAT/I3N, Department of Materials Science, NOVA School of Science and Technology, Universidade NOVA de Lisboa, 2829-516 Caparica, Portugal

[3] Laboratório Associado de Sistemas Inteligentes, LASI, 4800-058 Guimarães, Portugal

Abbreviations

C_{mct} (€)	The price of buying a machine tool
C_{mt} (€)	A machine tool's maintenance cost
$C_{tooling}$ (€)	The tooling cost such as cost of work holding devices and cutting tools
MC_{1kg} (€/kg)	The raw material (powder/wire/bar) cost per kilogram
EC_{1kWh} (€/kWh)	The electricity cost per kWh
$GC_{1m}{}^{3}$ (€/m^3)	The inert/shielding gas cost per cubic meter
$m_{material}$ (kg)	The quantity of raw material consumed, including waste

e_{part} (kWh)	The electricity consumed during product fabrication
g_{part} (m^3)	The total quantity of inert/shielding gas used
PPC_{1h} (€/h)	The hourly post-processing rate
LC_{1h} (€/h)	The operator cost per hour
$t_{available}$ (h)	The total time for which a machine tool is available
$t_{machine}$ (h)	The amount of time spent setting up, processing, and cleaning up a machine
$t_{post\text{-}processing}$ (h)	The total duration involved in post-processing operations
t_{labour} (h)	The amount of time required by the operator in carrying out all the necessary activities in part manufacture

1 Introduction

The industrial sector is one of the most resource intensive and polluting sectors accounting for shares over 40% in energy consumption [1], 20% in water withdrawals, and 18% in carbon emissions globally [2]. The growing awareness on adverse impacts of climate change such as increased greenhouse gas (GHG emissions) has led to formulation of different agreements by the public authorities such as the Kyoto Protocol [3], Paris Agreement [4], and European Green Deal [5] to mention few that set targets to reduce adverse environmental impacts. As a result, various countries have imposed stricter environmental legislations and financial penalties for their violations [6]. This pressure from public authorities and increased environmental consciousness among the customers has led to prioritization of sustainable manufacturing solutions to mitigate the negative impacts of their manufacturing operations, including their greenhouse gas emissions [7–9]. Sustainable manufacturing involves production of high-quality products and services that consume lesser resources like energy and material resulting in lower environmental emissions and costs [10]. Sustainable manufacturing can be realized by implementing different strategies like material efficiency, energy efficiency, design for sustainability, and predictive maintenance, among others [11].

Material efficiency is a fundamental strategy for sustainable manufacturing and involves reducing the use of primary materials without significantly altering the product's function or service [12]. Achieving high material efficiency is critical for transition to an environmentally friendly manufacturing as the production of just 5 key engineering materials (steel, cement, plastic, paper, and aluminium) is responsible for more than 50% of the industry sector's carbon emissions, with steel alone being responsible for 25% of the industrial carbon emissions [2]. Steel production is energy intensive and subsequently carbon intensive as most of it is carried out at elevated temperatures [13]. Material efficiency can be achieved using different strategies like part re-use, repair, resale, remanufacture, design for longer life, modularity, and dematerialization, among others [14].

In the context of metal fabrication, conventional subtractive manufacturing technologies such as computer numerical control (CNC) machining generate lot of material wastes due to material removal for manufacturing parts, limiting its environmental friendliness. Additive manufacturing (AM) technologies due to their capabilities of layer-by-layer fabrication of parts presents opportunities for achieving material efficiency through dematerialization, i.e. reduction in the amount of material consumed and wastes generated. AM technologies like powder bed fusion (PBF) and directed energy deposition (DED) are capable of processing metal feedstocks [15]. In laser powder bed fusion (LPBF) technologies, a powder bed is selectively fused using thermal energy of a laser or an electron beam, respectively. PBF technologies can build products with high accuracy but have slower build rates (2–10 g/min depending upon material) [16]. Slower build rates lead to higher energy demands, as demonstrated by Lunetto et al. [17]. Hence, material efficiency of PBF technologies can be overshadowed by their poor energy efficiency, adversely affecting its environmental friendliness. From an economic perspective, machine tools for PBF technologies are expensive [16, 18], limiting its implementation. Furthermore, PBF parts may exhibit anisotropy in mechanical properties, requiring further heat treatments to achieve even microstructure and mechanical properties [19]. In DED technologies, metal powders or wires are melted by focused thermal energy of a laser or electric arc and the molten material is deposited selectively. Powder-based DED technique has lower build rates resulting in longer build times, similar to PBF processes, and is used for building small accurate parts [20]. On the other hand, an emerging wire-based DED process of wire arc additive manufacturing (WAAM) has demonstrated the ability to fabricate higher build rates (50–130 g/min depending upon material) [16] and suitability for building large parts especially in shipping, energy, and construction sectors and need for cheaper machine tools [21, 22]. In WAAM, the feedstock metal wires are melted using an electric arc and deposited layer-by-layer using a robotic arm to build a desired product geometry (see Fig. 1a). However, WAAM technology presents challenges like prevalence of high residual stresses and distortions, poor accuracy, and surface finish, presence of defects like porosity, humping, cracks, and large grain growth in WAAM-fabricated parts that often lead to production of low-quality parts with inferior mechanical properties [23]. Therefore, post-processing finish machining operations are required to improve the dimensional accuracy and surface quality of WAAM parts [24], as demonstrated in

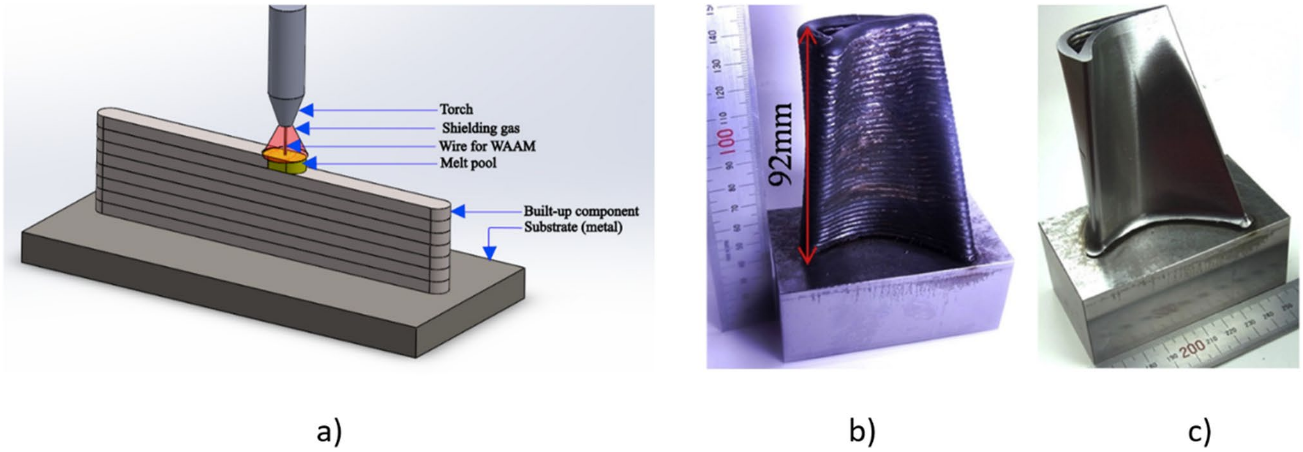

Fig. 1 **a** Schematic of WAAM process [26]; an example of WAAM part **b** as deposited; **c** after finish machining [27]

Fig. 1b, c. Additionally, heat treatment operations may be necessary to relieve residual stresses and refine the microstructure, thereby enhancing the mechanical properties of WAAM-built components [25]. However, the need for such post-processing operations increases the material, energy, and labour demands, negatively impacting the environmental and economic viability of WAAM compared to other manufacturing methods.

The interest among researchers about environmental impacts of metal additive manufacturing (MAM) processes has been growing in past few years. Kokare et al. [28] reviewed the present studies focused on environmental emissions of different MAM processes using LCA methodology and pointed out that powder bed fusion (PBF) processes such as laser powder bead fusion (LPBF) and electron beam melting (EBM) have been studied extensively compared to other MAM processes due to their better technological maturity and penetration in the industry. Several LCA studies on PBF manufactured functional industrial products such as automotive engines [29] and gears [30], aircraft components like brackets, seat buckles, engine covers, door hinge, and fork fitting [31], aeronautical turbine blades [32, 33], hydraulic components like valves [34], and washers [35] as well as biomedical femoral implants [36, 37]. Although PBF processes exhibited better material efficiency than conventional manufacturing (CM) processes, their energy requirements were significantly higher than CM processes. As a result, PBF processes were not seen environmentally friendly in some production cases like hydraulic washers [35] and gears [30] or did not result into substantial reductions in environmental impacts compared to CM, as in cases of automotive engines [29] and aeronautical turbines [32, 33]. For aircraft components [31], adoption of PBF processes was seen more environmentally friendly due to weight reduction enabled by these processes resulting in material savings during the manufacturing phase as well as fuel savings in subsequent use phase. In the case of femoral implants [36, 37], PBF was seen to be the most ecofriendly option as the positive impact of material savings outbalanced the negative impact of increased energy consumption. Hence, it can be inferred that compared to CM processes, PBF processes demonstrate lower material wastage but higher energy demand arising from its lower build rates [17]. Compared to PBF processes, the sustainability potential of directed energy deposition (DED) category of AM processes such as WAAM is understudied. Priarone et al. [38] compared energy consumption, manufacturing time, and costs of a steel beam, titanium bracket, and aluminium frame manufactured by WAAM and material removal processes. WAAM was observed to have lower energy requirement for all 3 components. However, WAAM was more expensive process for manufacturing steel beams and titanium brackets compared to machining processes due to its higher production time resulting from its post-processing operations. Bekker and Verlinden [39] performed an LCA of unit kilogram of stainless steel deposited by WAAM and compared its environmental impacts with green sand casting and CNC machining. WAAM was observed as the most environmentally friendly process, while CNC machining was reported to be the most environmentally damaging process causing an environmental impact 1.5 times greater than WAAM. Nonetheless, this study did not consider the effect of product geometry on environmental performance of a process. In another study, Shah et al. [40] observed that WAAM produced carbon steel and stainless steel I-beams result in 7 to 24% reductions in carbon emissions compared to conventional hot-rolled I-beams. Kokare et al. [41] assessed the ecological and economic impacts of a high-strength low-alloy steel (HSLA) wall manufactured by pure CNC milling, WAAM, and LPBF approaches. CNC machining was seen to be the most ecological and economic option for flatter walls. However, as the curvature of walls become more complex, WAAM was reported to be the most ecological as well as economic alternative. Similarly, Kokare et al. [42] and Pusateri et al. [43] demonstrated the environmental impact reduction enabled by WAAM in manufacturing of marine propellers. However, the calculations in the above studies [39–43] appear to be based on an intrinsic assumption that WAAM and conventionally fabricated parts guarantee similar mechanical performance. Hence, the mechanical performance of WAAM products need to be evaluated in addition to its environmental and economic impacts to select a manufacturing process holistically for a product. The above LCA studies of WAAM are summarized in Table 1.

After a careful analysis of above studies based on LCA of PBF and WAAM parts, the following literature gaps are realized: firstly, the scope of the LCA studies for WAAM [39, 40] neglected the post-processing finish machining that is required to eliminate the intrinsic surface waviness of fabricated products on their environmental impacts. Secondly, most of the current studies singularly focus on ecological performance of MAM technologies while ignoring their economic assessment. The cost incurred in manufacturing is one of the essential criteria for its adoption in the industry. Lastly, the existing studies do not assess mechanical properties of MAM parts. It is either implicitly or explicitly assumed that MAM parts have the same mechanical properties and guarantee identical performances compared to conventionally manufactured parts. As pointed out by Peng et al. [44], there is a need to integrate mechanical properties evaluation results in LCA studies of AM parts. Hence, such studies result into plain theoretical material, energy, or cost comparisons instead of holistic manufacturing technology comparisons that can help manufacturers select the most viable manufacturing process.

Therefore, the main objective of this study is to conduct a comprehensive environmental, economic, and mechanical characterizations of WAAM and compare it with more technologically mature subtractive CNC machining and additive LPBF technologies. In this paper, a process flow for WAAM technology along with its post-processing machining operations is established experimentally by fabricating a high-strength low-alloy (HSLA) geometry. Based on data from this experiment, environmental impact and cost assessments for WAAM are conducted using life cycle assessment and life cycle costing methodologies, respectively, and comparisons with LPBF and CNC milling approaches are carried out. Additionally, mechanical characterization of the fabricated WAAM part is also carried out. The outcomes of this comparative study can be helpful to AM specialists in the selection of the best cost, environment, and quality effective manufacturing route for their products.

The rest of the paper is structured as follows: Section 3 describes in detail the life cycle assessment (LCA), life cycle costing (LCC), and mechanical characterization methodologies to assess environmental impacts, costs, and mechanical properties, respectively. Section 3 demonstrates a case study performing environmental, economic, and mechanical assessments of a high-strength low-alloy steel part. The results of the case study are discussed in Section 4 and its conclusions are summarized in Section 5.

2 Methodology

This section discusses the different methodologies for environmental, economic, and mechanical assessment such as life cycle assessment (LCA), life cycle costing (LCC), and mechanical characterization techniques (uniaxial tensile testing and Vickers hardness), respectively, and their standards, frameworks, or steps of execution and experiments.

2.1 Life cycle assessment

Life cycle assessment (LCA) is a well-established procedure used to the compute environmental footprint of a product

Table 1 LCA studies of WAAM

LCA study	Functional unit	Findings
Priarone et al. [38]	Aluminium frame, titanium bracket, and steel beam	• WAAM consumed lower compared to CNC machining • The cost-effectiveness of WAAM was dependent upon processing times
Bekker and Verlinden [39]	1 kg stainless steel 316 product	CNC milling causes an environmental impact 1.5 times greater than WAAM
Shah et al. [40]	Carbon and stainless-steel beams	WAAM reported 7–24% lower carbon emissions than conventional hot rolling process
Kokare et al. [41]	High-strength low-alloy (HSLA) steel	WAAM was seen as environmentally and cost friendly only for walls with complex curvatures, compared to CNC machining
Kokare et al. [42]	HSLA marine propeller	WAAM showed 40% lower environmental impact and 8% lower cost relative to CNC milling
Pusateri et al. [43]	S355 and Inconel 625 boat propeller	• Adoption of WAAM can reduce the bronze demand by 8% • WAAM adoption along with Circular Economy strategy is more beneficial ecologically

over its partial or entire life span. The LCA is conducted based on its framework provided by "ISO 14044:2006-Environmental management—Life cycle assessment—Requirements and guidelines" standard [45] and is carried out following the steps illustrated in Fig. 2.

1. *Goal and scope definition*: This step involves determining the objective of the study, system boundaries, functional unit, environmental impact assessment method, environmental impact categories, assumptions, and limitations of the study
2. *Life cycle inventory analysis*: In this step, the life cycle inventory data like raw materials, energy, and wastes, among others, linked with each life cycle stage of the product analysed are compiled. The sources for these data include experimental measurements, different LCA databases, scientific literature, and public reports, to name a few
3. *Life cycle impact assessment*: Here, a life cycle model of the product under investigation is created based on the life cycle inventory data collected in the LCA software package. Then, different environmental impacts such as global warming, eutrophication, acidification, and water footprint, among others, are computed using the characterization factors of the LCA method chosen
4. *Interpretation*: This stage involves analysing the results of life cycle impact assessment, identifying different environmental hotspots, and making recommendations to decrease the environmental impacts and improve the product's life cycle performance

2.2 Life cycle costing

Life cycle costing (LCC) methodology is used to compute cost of a product for its partial or entire life cycle and is effective in making decisions to minimize the cost of a product without compromising customer requirements [46]. While there are multiple standards [46, 47] and cost models to conduct a LCC study, no particular methodology has been considered as a standard because of distinctions in user inclinations, problem type, and data collection systems [48]. Moreover, considerable background efforts are required in determining the cost driven activities and resources, obtaining their costs through quotations or other relevant sources, in addition to selecting the most appropriate cost model in the given context. Hence, a well-organized, step-by-step LCC approach needs to be developed so that the cost assessment can be completed in a successful and time efficient manner. Greene and Shaw [49] have proposed a 10-step generic and effective LCC framework that (refer to Fig. 3). Owing to the proper organization, ease of implementation, and flexibility to adapt this approach for a given problem statement, this LCC framework is used in conducting a cost assessment in this study.

As seen from Fig. 3, the first step in LCC analysis is determining the purpose of the analysis, such as cost comparisons, budget estimation, or cost–benefit analysis. Then, by choosing the required systems and subsystems, the analysis's scope is established. Depending upon the objective of the LCC study, the best suitable LCC model and cost estimating technique are selected. After gathering pertinent information from several sources, inputs to the LCC model are created. Additionally, their consistency, correctness, validity, and completeness are examined. In order to represent cost ranges with variations in input parameters,

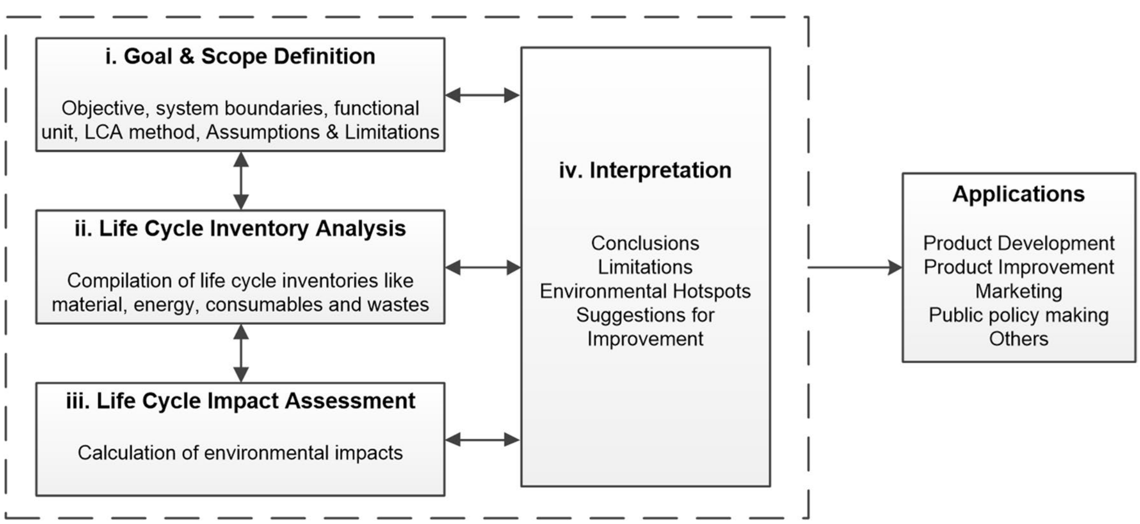

Fig. 2 Life cycle assessment framework based on ISO 14044 standard [45]

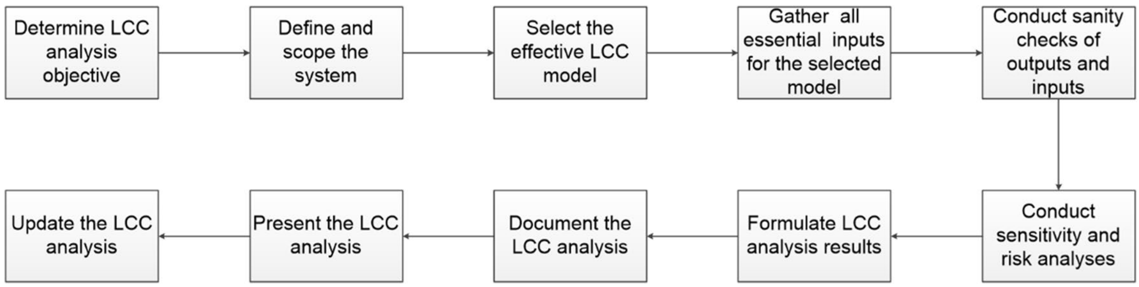

Fig. 3 LCC framework adapted from [49]

sensitivity and risk evaluations are also carried out. Next, the outcomes of the LCC analysis are examined, cost factors are recognized, and the most appropriate options are chosen and defended. The analysis is then presented to the intended audience, documented, and needs to be updated with changes in cost data.

2.3 Mechanical characterization

Mechanical characterizations are standardized tests used to identify the mechanical characteristics of a material or product in a specific environment, and they are a vital aspect of any design and/or manufacturing process. Mechanical characterizations are performed to assure safety by understanding a material's working limits, aiming to prevent catastrophic failures, to establish compliance, to minimize costs, to offer proof of concepts to clients, and finally to drive product improvements [50]. This enables engineers to select the most appropriate material for a given application.

The surface integrity of the finish machined WAAM part was characterized by measuring its average surface roughness (Ra) using a Mahr MarSurf PS 10 mobile roughness measuring device in accordance with ISO 21920–2:2021 standard [45]. The Ra was measured three times in five equally spaced sections on the sample and the average of recorded values is calculated to determine the surface roughness of the machined WAAM part.

The mechanical properties of the WAAM part built in this work, including ultimate tensile strength (UTS), yield strength (YS), and elongation at break, were evaluated by performing uniaxial tensile testing (UTT) in accordance to ASTM E8/E8M standard [51]. A total of four samples, two samples each in horizontal and vertical orientations parallel and perpendicular to the deposition direction, respectively, from a WAAM-fabricated high-strength low-alloy steel (ER70S) wall were cut and machined to the required dimensions as shown in Fig. 4. The tensile tests were carried out using a displacement rate of 1 mm/min.

Vickers microhardness tests were carried out in accordance with ISO 6507–1:2023 standard [52] using a Mitutoyo HM-112 Vickers Hardness Testing Machine for samples in horizontal and vertical directions. The hardness indentations were made using a load of 0.5 kgf for 10 s. A sample length of 20 mm was tested with a distance of 200 µm between two successive indentations.

Additionally, microstructural characterization of the WAAM samples was performed using a Leica DMI5000 M inverted optical microscope to study the correlation between mechanical properties and microstructure obtained for WAAM samples in this study.

3 Case study

This section analyses the manufacturing costs and environmental footprints of CNC machining, LPBF, and WAAM. Here, a high-strength low-alloy steel component with a modestly complicated shape, as seen in Fig. 5, was fabricated. Its surface area is approximately 75 cm^2, and its volume is roughly 23 cm^3. This part weighs about 181 g when one considers the density of steel as 7.8 g/cm^3.

3.1 Goal and scope definition

The purpose of this study is to evaluate and compare the environmental footprint and costs incurred during the manufacture of a given product using WAAM, LPBF, and pure CNC machining methods. The study is being conducted to identify the most sustainable process, both economically and environmentally. Based on the findings of this study, AM practitioners will be able to select the most environmentally benign and cost-effective option for manufacturing comparable products, allowing them to maximize productivity and cost efficiency. The system boundaries of this study are outlined in Fig. 6. The steps involved in each manufacturing approach are explained in detail in Section 3.2.

3.2 Life cycle inventory analysis

This section describes in-depth life cycle inventory (LCI) analysis for WAAM, LPBF, and CNC milling approaches where the quantities of different life cycle inventories such

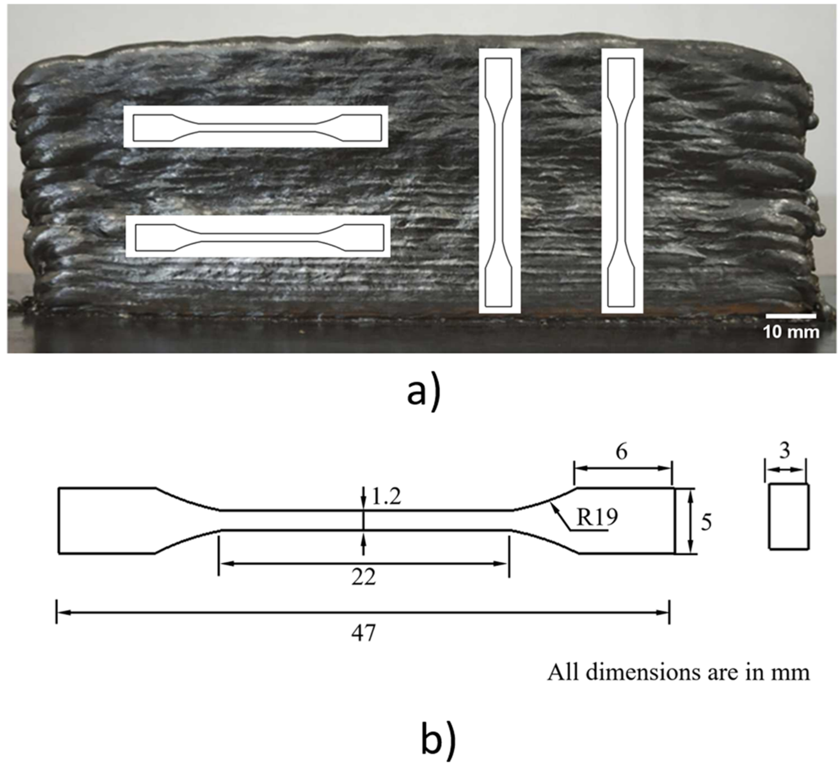

Fig. 4 **a** Orientation of tensile test samples and **b** their dimensions

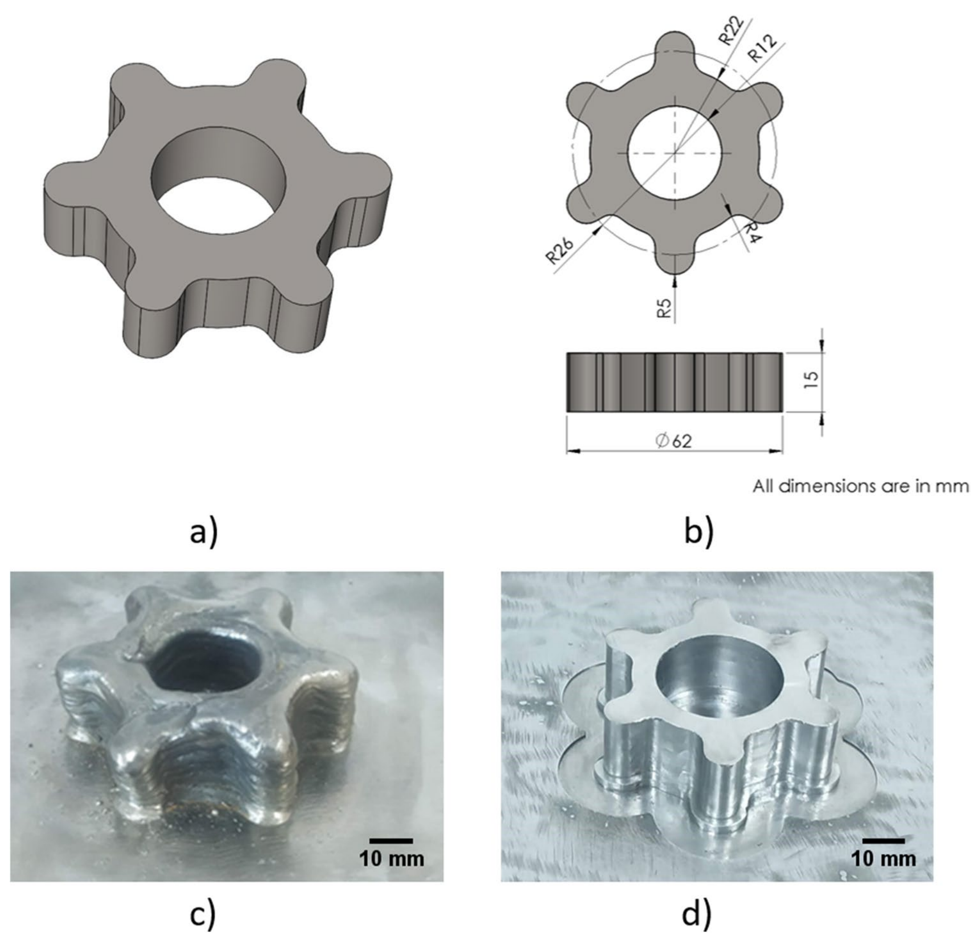

Fig. 5 **a** Part considered in this study; **b** its dimensions; **c** as deposited WAAM part; **d** WAAM part after finish machining

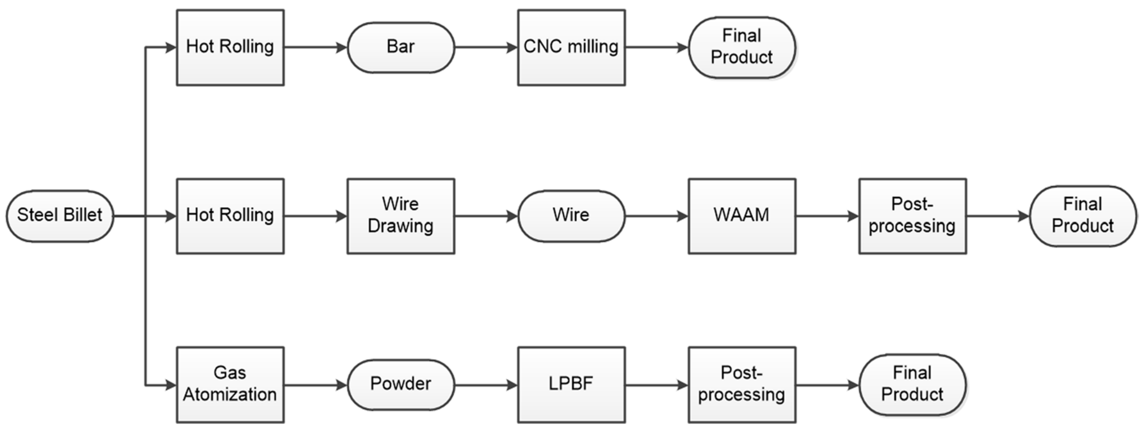

Fig. 6 System boundaries considered in this considered

as raw material, energy, shielding gas, and compressed air, among others, are determined based on experimental measurements, calculations based on scientific literature, and data taken from the existing LCI databases.

3.2.1 WAAM

The WAAM-based approach starts with the manufacture of the raw material, feedstock wire. Typically, steel billets are hot rolled and then wire drawn to produce feedstock wire. The life cycle inventory data for hot rolling and wire drawing stages is taken from the Ecoinvent 3 database. The hot rolling and wire drawing stages are considered to have a material waste rate of 5% and 4%, respectively, based on this database. During WAAM deposition, a wire feed speed of 3 m/min and travel speed of 360 mm/min were used as process parameters resulting in a layer height of 1.5 mm. As a result of these parameters, it took nearly 15 min for the projected part to be printed. A cooling period of 2 min is allowed between two consecutive layers. To keep the molten pool free from atmospheric interactions, a shielding gas composed of 82% argon and 18% CO_2 is used at a flow rate of 16 L/min. The energy utilized during WAAM is determined based monitoring of voltage (V) and current (I) using a NI USB 6008 data acquisition device and the LabView software, as illustrated in Fig. 7. The total energy consumed during WAAM is the summation of energies consumed during melting and deposition of molten wire ($E_{\text{deposition}}$), as well as for the duration where machine is idle, i.e. set-up and interlayer cooling time ($E_{\text{stand-by}}$).

$$E_{WAAM} = E_{stand-by} + E_{deposition} \tag{1.1}$$

The energies for each phase are calculated by multiplying their power requirement and time consumed for each phase as follows:

$$E_{WAAM} = P_{stand-by.}\left(t_{set-up} + t_{cooling}\right) + P_{deposition.}t_{deposition} \tag{1.2}$$

Fig. 7 WAAM power measurement

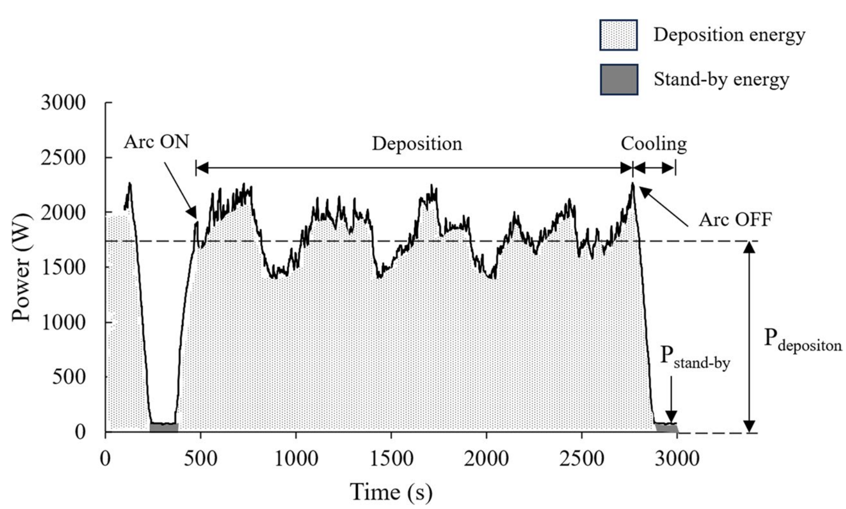

The dimensions of as-deposited WAAM products are frequently not accurate due to wavy surfaces and poor process precision, resulting in the need for finishing machining. Therefore, the WAAM-built product was given an adequate material allowance across its surface area to allow for material removal during finishing. The CAD model of the part was adjusted to include a 2-mm machining allowance across its entire surface area. In addition, a CAD model of the as-deposited WAAM part was built by 3D scanning it, in order to capture its surface waviness and (eventual) distortions. In the CAM software, this 3D-scanned CAD model served as the stock material for simulating the post-processing machining process. The post-processing finish machining for the WAAM part was carried out in three operations, with the following cutting velocity (V_c), feed per tooth (f_z), and depth of cut (a_p): face milling of the top surface ($V_c = 122$ m/min; $f_z = 0.01$ mm, $a_p = 1$ mm), followed by pocket milling of the central hole and contour milling of the peripheral edges ($V_c = 62$ m/min; $f_z = 0.01$ mm, $a_p = 4$ mm for both conditions). A face milling cutter of 50 mm diameter made up of high-speed steel and an endmill of tungsten carbide of 8 mm diameter and 4 cutting teeth are used in face milling and contour milling, respectively. The total cutting time observed was 54 min. Moreover, a setup time of 15 min was also considered. The energy for post-processing machining is calculated based on the power monitoring of the machining process using the above cutting parameters as depicted in Fig. 8.

From Fig. 8, three phases in machining can be identified as follows: (i) stand-by phase, where the CNC milling machine is idle during set-up and clean-up activities; (ii) air-cutting phase, where the cutting tool is approaching the workpiece, moving in air but not removing material; and (iii) cutting phase, where the cutting tool removes the material from the workpiece. Therefore, the total energy consumed in machining ($E_{\text{CNC-milling}}$) is the summation of energies consumed in stand-by ($E_{\text{stand-by}}$), air-cutting ($E_{\text{air-cutting}}$), and cutting (E_{cutting}) modes as follows:

$$E_{CNC-milling} = E_{stand-by} + E_{air-cutting} + E_{cutting} \tag{1.3}$$

The energies for each phase are calculated by multiplying their power requirement and time consumed for each phase as follows:

$$E_{CNC-milling} = P_{stand-by}.t_{set-up} + P_{air-cutting} + P_{cutting}.t_{cutting} \tag{1.4}$$

The overview of steps involved in fabrication of the part using WAAM is depicted in Fig. 9. Table 2 lists the complete environmental inventories for each phase of the WAAM process.

3.2.2 CNC milling

CNC machining approach begins by rolling the steel billet into a cylindrical bar. The inventory data for the steel billet and hot rolling have been derived from the Ecoinvent 3 database [53]. This database estimates the material utilization of hot rolling to be nearly 95%. In this scenario, a cylindrical bar measuring 70 mm in diameter and 17 mm in height is considered as the workpiece. Firstly, the top surface is face milled using a high-speed steel face milling cutter of 50 mm in diameter. Then, with an 8-mm endmill with four cutting edges, the workpiece is then machined to the required geometry by pocket milling of the central hole and contour milling of peripheral edges. The cutting parameters

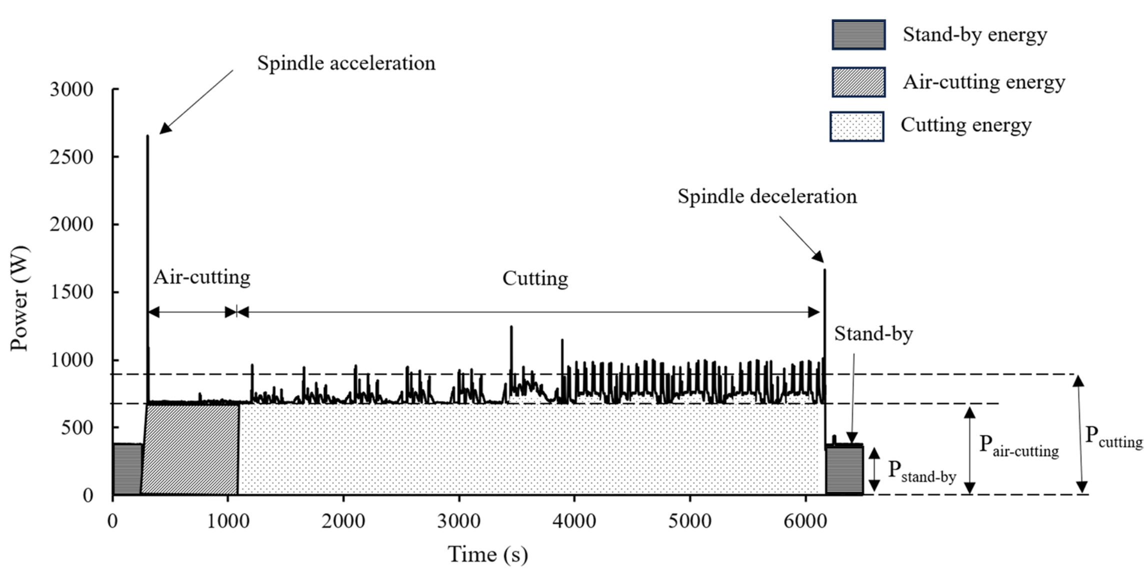

Fig. 8 CNC machining power measurement

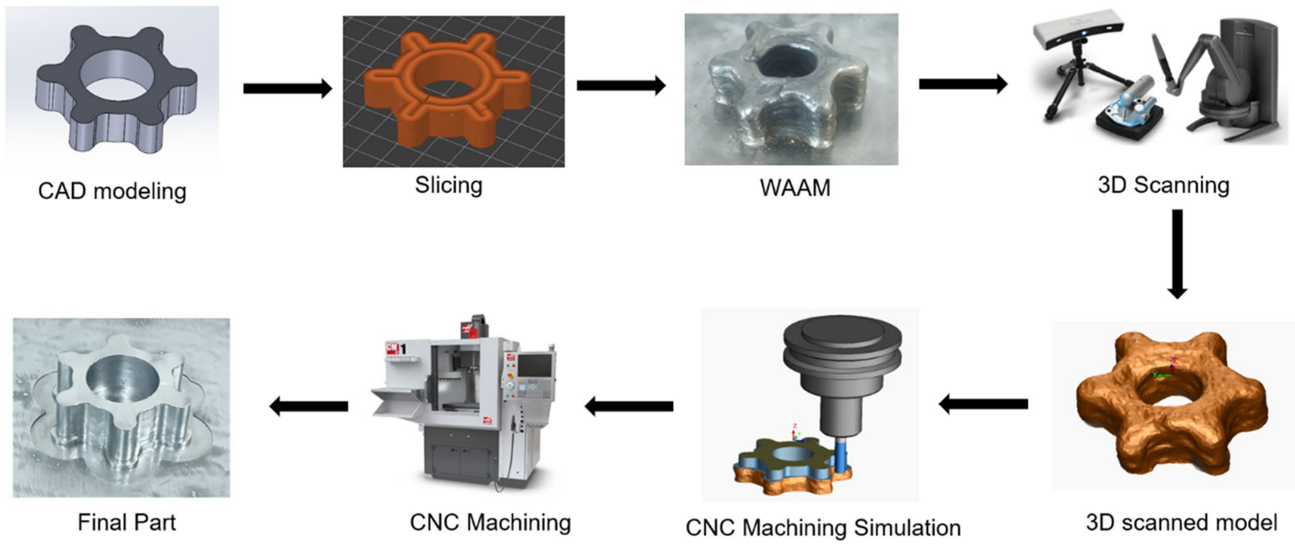

Fig. 9 Steps involved in WAAM of the selected part

Table 2 Life cycle inventories for WAAM

Inventories	Quantity	Source
Raw material production		
Steel billet	0.329 kg	Based on Ecoinvent 3 database
Hot rolling	0.329 kg	Based on Ecoinvent 3 database
Wire drawing	0.314 kg	Based on Ecoinvent 3 database
WAAM		
Steel wire	0.302 kg	Measured
Energy	0.47 kWh	Measured
Shielding gas	0.23 m^3	Calculated by multiplying gas flow rate and printing time
Post-processing		
Milling chips	0.121 kg	Measured
Electricity	0.729 kWh	Measured

considered are as follows: face milling ($V_c = 122$ m/min; $f_z = 0.01$ mm, $a_p = 1$ mm) and pocket and contour milling ($V_c = 62$ m/min; $f_z = 0.01$ mm, $a_p = 4$ mm). Based on the cutting process simulations in SolidWorks CAM, the entire cutting process lasts for 85 min. In addition, 15 min are considered for machine set up. The CNC machining route exhibits a material efficiency of about 35%. The energy for CNC milling approach is calculated in the same way as that for post-processing machining in the WAAM approach. The CNC milling approach consumes a total energy of 1.14 kWh. The environmental inventories of this route are comprehensively enlisted in Table 3.

Table 3 Life cycle inventories for CNC milling

Inventories	Quantity	Source
Raw material		
Steel billet	0.537 kg	Taken from Ecoinvent 3 database
Hot rolling	0.537 kg	Taken from Ecoinvent 3 database
CNC milling		
Workpiece	0.51 kg	Calculated
Material wastes	0.329 kg	
Electricity	1.14 kWh	Measured

3.2.3 LPBF

The LPBF route begins with the production of metal powder. Gas atomization is the process used to produce metal powder. A high velocity speed stream of argon gas fragments the molten metal billets through gas atomization, and metal powder is formed when these particles are cooled. The data for life cycle inventories of gas atomization were acquired from a preceding study by Peng et al. [34] including the gas atomization of stainless steel. According to this study, 85% of the input material to the gas atomization process can be converted into powder, with an energy consumption of 2 kWh/kg. Furthermore, the process consumes 280 L of water and 3.5 Nm^3 of Ar gas per kilogram of powder created. The following process parameters are considered for LPBF in accordance with studies involving manufacturing of steel-based parts [30, 35]: a laser scan speed of 1100 mm/s, a hatch distance of 100 µm, and a layer thickness of 50 µm, resulting in a material deposition rate of 19.8 cm^3/h. A 7-s recoating period is maintained between consecutive layers. Generally, LPBF produces better surface finishes of less than 50 µm [54], so a constant machining allowance of 1 mm throughout the part's surface area is allowed based on a study by Ingarao et al. [55]. Furthermore, a material allowance of 10% of the part weight is also applied during printing to construct the support structures, as calculated using Prusa's 3D slicer. The resource consumption measurements performed by Gebbe et al. [56] for LPBF of stainless steel powder were used to calculate electricity, compressed air, and Ar gas required for the process. During LPBF, five different operation modes are seen in the following order: (i) preparation of the LPBF machine, (ii) preheating of the machine chamber and flooding of argon to create an inert atmosphere, (iii) exposure of laser to selectively melt the powder, (iv) recoating with a fresh powder, and (v) cooling down of the produced part. Hence, the energy expended during LPBF is the sum of energies consumed in individual operation modes:

$$E_{LPBF} = E_{preparation} + E_{pre-heating} + E_{exposure} + E_{recoating} + E_{cooling} \tag{1.5}$$

The energies in each operation mode can be expressed as product of corresponding power requirement and time as follows:

$$E_{LPBF} = P_{preparation}.t_{preparation} + P_{pre-heating}.t_{pre-heating} + P_{exposure}.t_{exposure.} + P_{recoating}.t_{recoating} + P_{cooling}.t_{cooling} \tag{1.6}$$

Table 4 displays the calculated energy, gas, and compressed air values for each of the steps involved in LPBF.

LPBF post-processing operations similar to WAAM are considered, such as face milling ($V_c = 122$ m/min; $f_z = 0.01$ mm, $a_p = 1$ mm), succeeded by pocket milling and contour milling ($V_c = 62$ m/min; $f_z = 0.01$ mm, $a_p = 4$ mm). In total, the post-processing process takes 49 min based on the machining processes simulated in SolidWorks CAM. For post-processing energy, the power requirements for different modes are identical to that of WAAM as similar cutting tool and parameters are considered. The post-processing energy is calculated by multiplying power requirements for different machining modes with their respective times. Table 5 summarizes the inventories utilized in the LPBF process.

3.3 Cost model

The cost model used to compute the production costs for CNC milling, WAAM, and LPBF developed previously by the authors [41] is used for economic assessment in this study. This model considers the following costs:

- Machine cost ($C_{machine}$): The machine cost includes both the purchase and tooling costs as well as the cost of its maintenance for each manufacturing approach examined
- Material cost ($C_{material}$): This is the cost incurred as a result of the use of raw materials, such as metal wire, powder, and bar in the case of WAAM, LPBF, and CNC milling, respectively

Table 5 Life cycle inventories for LPBF

Inventories	Quantity	Source
Raw material		
Steel billet	0.319 kg	Taken from Ecoinvent 3 database
Gas atomization		
Energy	0.638 kWh	Based on Peng et al. [34]
Inert gas (argon)	1.11 Nm^3	Based on Peng et al. [34]
Water	89.32 L	Based on Peng et al. [34]
LPBF		
Steel powder	0.271 kg	Computed based on 10% material allowance for building supports
Energy	8.75 kWh	Based on Gebbe et al. [56]
Compressed air	2.51 m^3	Based on Gebbe et al. [56]
Argon	1.2 m^3	Based on Gebbe et al. [56]
Post-processing		
Machining chips	90 g	Estimated based on 1 mm constant machining allowance
Energy	0.498 kWh	Calculated

Table 4 The calculated energy, gas, and compressed air values for each of the steps involved in LPBF.

LPBF production mode	Time (h)	Electricity		Compressed air		Argon	
		Power (kw)	Energy (Kwh)	Flow rate (L/min)	Total (m^3)	Flow rate (L/min)	Total (m^3)
Preparation	0.50	0.363	0.18	0	0.00	0	0
Pre heating	0.50	2.523	1.26	0	0.00	40	1.2
exposure	1.79	2.625	4.70	16.7	1.79	0	0
recoating	0.72	2.625	1.89	16.7	0.72	0	0
Cooling	2.00	0.363	0.73	0	0.00	0	0
Total	5.51		8.75		2.51		1.2

- Consumables cost ($C_{\text{consumables}}$): In addition to the raw material cost, the costs of consumables essential for each manufacturing approaches, such as energy, inert gas (in the instance of AM technologies), or coolant (in the instance of CNC milling) are also included in this model
- Post-processing cost ($C_{\text{post-processing}}$): This includes costs related to post-processing operations include machines, consumables, and labour. This cost is applicable only for AM technologies
- Labour cost (C_{labour}): There are several activities the operator has to carry out in order to implement each manufacturing approach. These activities include preparation, setup, processing, post-processing, and cleaning up the site after the process has been completed. Hence, the cost of operator incurred in executing these activities has also been included in the cost model

Therefore, the production cost ($C_{\text{production}}$) is calculated as the sum of above individual costs as follows:

$$C_{production} = \left(\begin{array}{l} \underbrace{\left(\left\{C_{mct} + C_{mt} + C_{tooling}/t_{available}\right\} \times t_{machine}\right)}_{C_{machine}} + \underbrace{m_{material} \times MC_{1kg}}_{m_{material}} + \underbrace{e_{part} \times EC_{1kWh} + g_{part} \times GC_{1m3}}_{C_{consumables}} + \\ \underbrace{PPC_{1h} \times t_{post-processing}}_{C_{post-processing}} + \underbrace{LC_{1h} \times t_{labour}}_{C_{labour}} \end{array} \right) \quad (1.7)$$

3.4 Economic inventory

Three shifts of 8 h each, two hundred and fifty working days per year, and a 7-year depreciation period are assumed for each machine tool use. According to our calculation, the machine was available 80% of the time available for use. According to the quotations provided by vendors, the costs of LPBF equipment, WAAM machine tool, and CNC machine are respectively 500,000 euros, 300,000 euros, and 150,000 euros. Additionally, 3% of the machine tool cost is spent on maintenance and 2% on tooling each year. Consequently, the total costs of the LPBF, WAAM, and CNC milling machines are 20 €/h, 12 €/h, and 6 €/h, respectively, as a result of the above factors. The price of 1 kg of steel wire is around 16 euros. The price of steel bar for CNC milling is around 5 euros per kilogram, and the price of steel powder is around 33 euros for each kilogram, corresponding to supplier quotations. Portugal's electricity prices are 0.13 euros per kilowatt hour [57]. The shielding gas is priced per meter at 2.3 euros, according to a quotation provided by the supplier. Throughout this study, labour costs are calculated at 15 €/h [58]. Table 6 gives a comprehensive summary of the economic inventories collected for this study.

Table 6 Economic inventory analysis

Costs	WAAM	CNC milling	LPBF	Reference
Machine cost (€/h)	12	6	20	Calculated
Material cost (€/kg)	16	5	33	Quotation
Electricity cost (€/kWh)	0.13	0.13	0.13	[57]
Inert gas/shielding cost (€/m^3)	2.3	2.3	2.3	Quotation
Post-processing cost (€/h)	21	-	21	Calculated
Labour cost (€/h)	15	15	15	[58]

4 Results and discussion

In this section, the comparative results of environmental, economic, and mechanical characterizations are discussed. The major drivers of environmental and economic impacts are identified for each process. The effect of variables like production volume and product volume on environmental and economic behaviour are studied. Additionally, the mechanical strength and hardness imparted by WAAM process is also compared to those of the parent material.

4.1 Environmental impact assessment

For the assessment of the environmental impact of CNC milling, WAAM, and LPBF, ReCiPe 2016 (Hierarchist) is used. Based on the ReCiPe 2016 Midpoint (Hierarchist) method, an assessment of the environmental footprint expressed in eighteen different categories of environmental emissions, such as global warming, acidification, particulate matter formation, ozone depletion, and eutrophication, among others, is conducted. Figure 10 displays the relative environmental impact comparisons for WAAM, CNC milling, and LPBF in relative terms, based on the results from the ReCiPe midpoint assessment. The environmental emissions calculated in 18 different environmental indicators for WAAM, CNC milling, and LPBF are listed in the Appendix at the end of this paper.

For better comparison, the result of all environmental footprint categorizes are transformed into a single score. This is done by applying a weighing method in the ReCiPe 2016 Endpoint (H) method of the environmental impact assessment to translate the scores of these 18 environmental

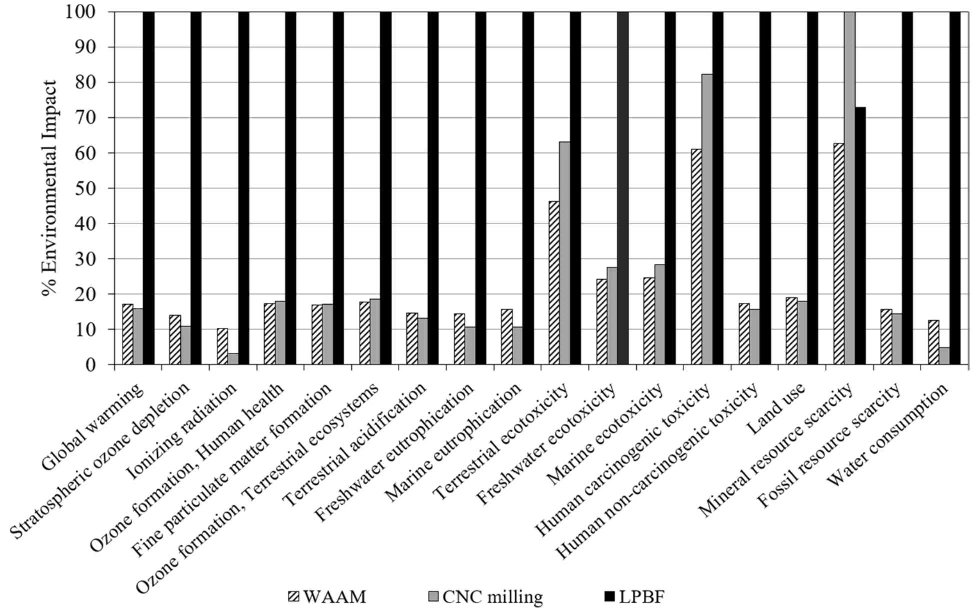

Fig. 10 ReCiPe midpoint assessment results

impact categories into a single numerical score (stated in milli eco-points or simply milli points (mPts)). Figure 11 illustrates the results of the ReCiPe endpoint of the study.

As seen from Fig. 11, the WAAM approach is observed to the least environmentally damaging with 116 mPts, followed by CNC milling (126 mPts) and LPBF (511 mPts). Additionally, the uncertainties in the overall environmental impacts were also computed using Monte Carlo simulations. Here, each inventory input was assumed to have a standard deviation of ± 10% of the baseline value, following a normal distribution. The LCA models were simulated for 10,000 iterations. The ecological impacts for WAAM, CNC milling, and LPBF vary in the ranges of 103–129 mPts, 107–145 mPts, and 459–562 mPts, respectively.

Each inventory input is also examined in terms of its contribution to the overall environmental impact. A summary of these results is shown in Fig. 12. The steel billet contributes a majority of 51% of the overall ecological burden of the WAAM approach. Another important contributor is the shielding gas that accounts for 20% of the overall impact. The post-processing, i.e. finish machining, accounts for nearly 13% of the overall environmental impact. The electrical energy used for material deposition, wire drawing, and hot rolling possess minor contributions of 7%, 6%, and 3%, respectively. Similar to WAAM, the steel billet is the foremost ecological hotspot for CNC machining methodology, accounting for about 75% of the total environmental impact. A further 19% of the overall environmental burden of this process is incurred by the energy consumed in the machining process, while the hot rolling process represents 5% of the total impact. As far as LPBF is concerned, its primary environmental impact is due to the energy consumed during the process, which contributes 36% to the overall ecological impact. The inert gas consumption results in 26%, while gas

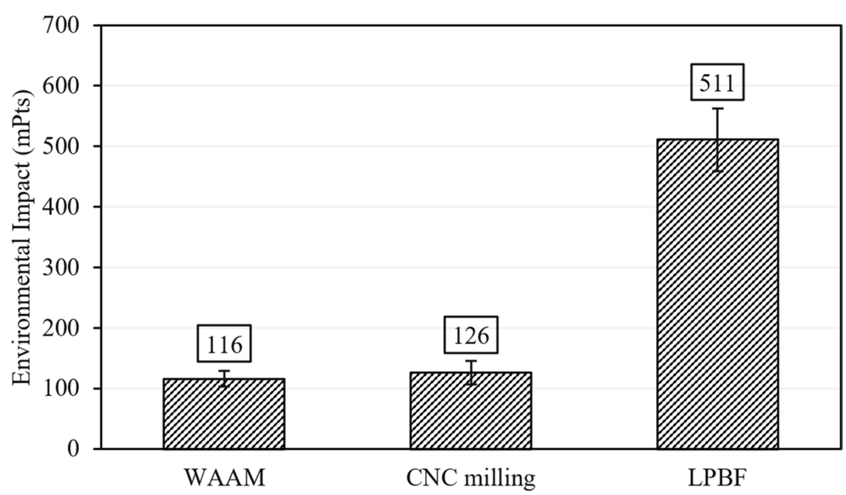

Fig. 11 Single score environmental impact assessment

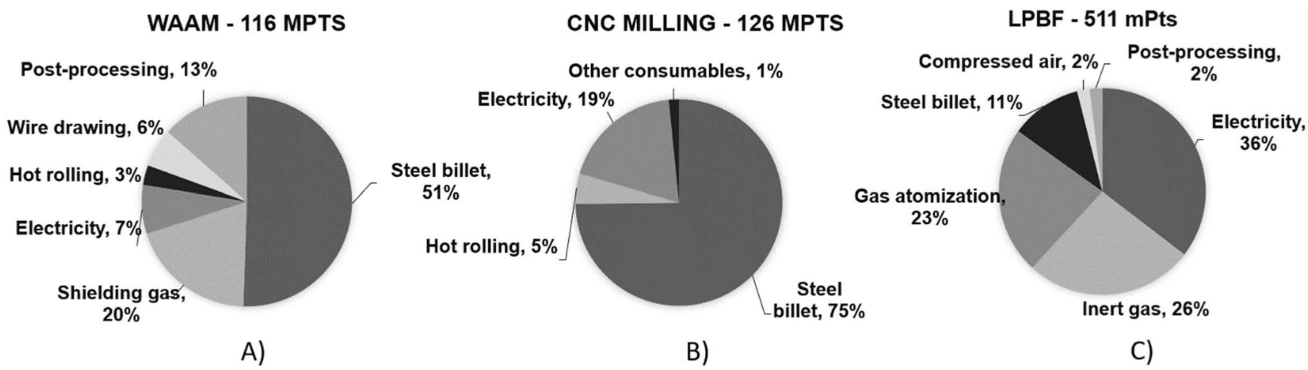

Fig. 12 Life cycle inventory wise breakdown analysis for **A** WAAM, **B** CNC milling, **C** LPBF

atomization accounts for 23% of the environmental impact. Although steel billet production alone accounts for 11% of the environmental impact, raw material production, i.e. steel billet production along with gas atomization, accounts for a third of the total impact. The post-processing stage and compressed air intake in LPBF contribute to a small extent (2% each).

4.2 Cost assessment

For each manufacturing approach, production cost is calculated using the economic data gathered and the cost model described earlier. The WAAM approach costs 53.5 €, a CNC approach costs 38 €, and a LPBF approach costs 232 € (see Fig. 13). Similar to the environmental assessment, the influence of uncertainties in each cost input were quantified using Monte Carlo simulations by considering a standard deviation of ± 10% and normal distribution for each cost input. Consequently, the production costs for WAAM, CNC milling, and LPBF lie in the intervals of 38–71 €, 32–44 €, and 199–267 €, respectively. Based on these three approaches examined, CNC milling appears to be the most economical approach. The cost of labour is the biggest contributor to CNC machining cost, accounting for 66% of the total product cost. The machine cost is second at 27%, followed by material cost at 7% contribution. In the WAAM, almost 45% of the production costs are attributed to the post-processing stage that involves finish machining of the as deposited WAAM part. The post-processing costs involve the costs associated with CNC milling machine, its maintenance and tooling, machining consumables like energy, cutting fluid, and cutting tools, and the labour involved. Labour for WAAM contributes 25% of the unit cost, while machine costs contribute 20%. Material cost comprise 9% of unit costs while consumables play a negligible role (1%). A key cost driver in the LPBF approach is machine cost, which causes 48% of the total production costs. There is also a significant contribution from labour costs (37%) to the production cost while the post-processing finish machining operation contributes to 7% to the production cost. The cost of raw material, i.e. metal powder used in LPBF, constitutes only 4% of the total production cost, owing to superior material efficiency of LPBF. Additionally, consumables such as energy and inert gas also contribute 4% each to the total production cost of LPBF.

Fig. 13 Cost assessment results

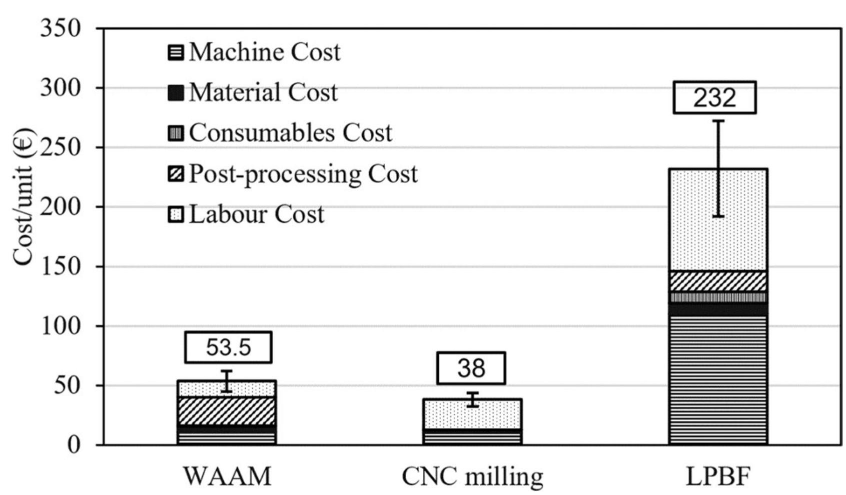

4.3 Effect of production volume

In the above cost analysis, the costs associated with production of a single part are analysed. As the considered part is small and medium in complexity, economies of scale can be achieved to reduce its production cost by increasing the production. Therefore, the effect of production volume on the product cost has also been studied by varying the batch size from 1 to 50 as illustrated in Fig. 14. Overall, it is observed that the production cost for all three approaches decreases with increase in batch sizes. This is attributed primarily to the better utilization of the machine tools, due to lowering of machine idle time (preparation, set up, and cooling times) per part production. This in turn reduces the machine and labour costs associated with each approach. For batch sizes above 25, the unit production cost stabilizes at about 123 € for LPBF, 34 € for CNC machining, and 31 € for WAAM approaches. While CNC machining is the most economical choice for single unit production, WAAM is realized to be the most cost-friendly option for batch sizes above 3.

4.4 Effect of product volume

As mentioned previously, WAAM has demonstrated very high deposition rates (up to 10 kg/h) enabling it to fabricate large-scale real-life components (> 10 kg) with low and medium complexity in relatively shorter times [22]. However, in this study, a small mechanical part weighing < 200 g was fabricated using WAAM owing to the academic nature of this research and limited laboratorial space. Nevertheless, the environmental and economic sustainability of WAAM in fabricating large-scale products is also examined in this study by uniform scaling (about centroid, in X, Y, and Z directions) of the considered part geometry up to a factor of 5 times its original size. The environmental and cost assessments of these upscaled part versions are conducted based on the environmental and economic inventories collected previously. As the product geometry is scaled up to 5 times, its volume gets magnified by 125 times. In this study, a lateral material margin of 2 mm was seen to sufficient to eliminate WAAM's surface waviness during post-processing material removal. This resulted in material efficiency of 60% for WAAM. However, as the part is scaled up, this material removed during the post-processing becomes a smaller fraction of the overall raw material consumed. Hence, higher material efficiency than CNC milling of around 90% can be obtained by WAAM for the larger version of product scaled up by a factor of 5 (refer to Fig. 15a). Owing to this better material efficiency, WAAM approach needs about half the primary raw material (steel billet) consumed in CNC milling for fabricating a 5 times larger version of the product, as seen in Fig. 15b). As a consequence of these material savings, WAAM can cause nearly half the environmental impact (refer to Fig. 15c) and reduce the production cost by 40% (see Fig. 15d) for fabricating a 5 times larger version of this part due to shorter manufacturing time, when compared to CNC milling approach. Hence, based on the above analysis, it can be concluded that WAAM is more effective than conventional CNC machining in terms of environmental and economic sustainability for manufacturing large-scale products.

The above analysis compared the environmental impacts and costs associated with production of a component by WAAM and conventional CNC machining. The environmental and cost effectiveness of WAAM can be further leveraged by utilizing WAAM for remanufacturing and repair of worn-out components [59, 60]. Priarone et al. [59] investigated the potential of hybrid WAAM and CNC milling based approach to repair worn out H13 steel mold inserts used for casting of aluminium cylinder heads in internal combustion engines. It was seen that this hybrid WAAM and CNC milling based repair approach could extend the life cycle of the mold over 5 times, resulting in substantial energy and material savings compared to substitution of worn-out mold with a new

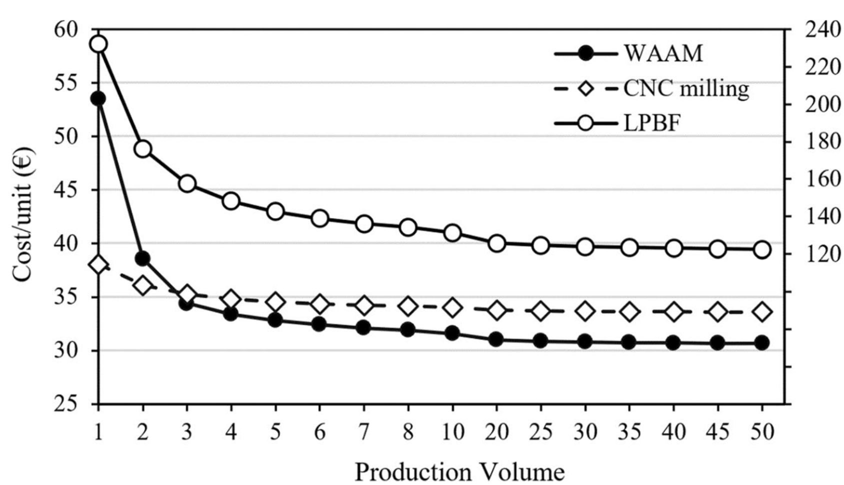

Fig. 14 Effect of production volume on cost/unit for WAAM, LPBF, and CNC milling approaches

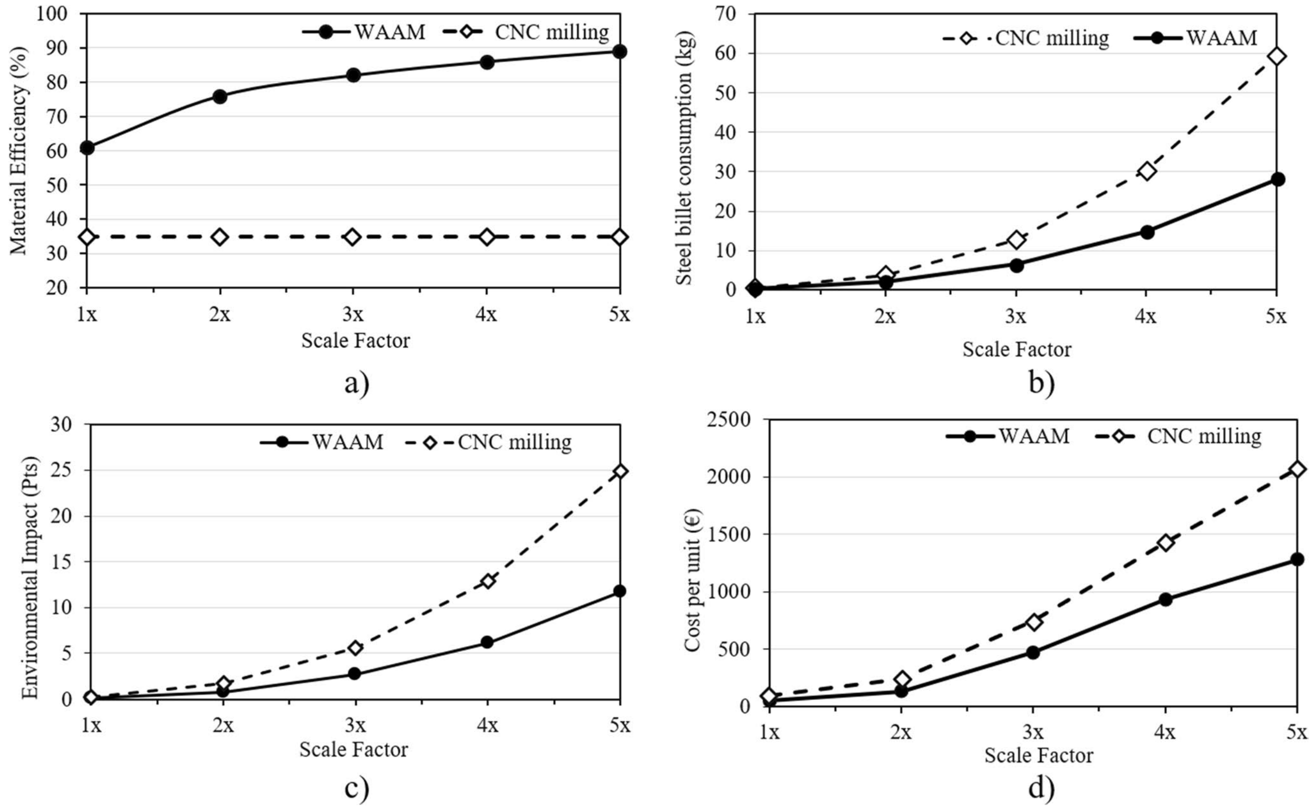

Fig. 15 Effect of scaling up of part on **a** material efficiency, **b** steel billet consumption, **c** environmental impact, and **d** unit product cost for WAAM and CNC milling approaches

CNC machined mold. Pagone et al. [60] explored the use of WAAM to repair a steel driver disk by redepositing metal on its worn-out areas. The findings showed that using WAAM based repair eliminated the need to manufacture an entirely new driver disk, which led to substantial reductions in both energy use and carbon emissions. Hence, by focusing on repairing only the damaged areas rather than producing a new component from scratch, WAAM can be much more cost-efficient and environmentally friendly.

4.5 Mechanical characterization results

4.5.1 Surface roughness test

The average surface roughness of the machined WAAM part were measured following the ISO 21920–2:2021 standard [61]. The average surface roughness (Ra) obtained for the machined WAAM surface is 0.855 ± 14 μm (refer to Fig. 16). Kaynak and Kitay [62] observed a surface roughness of 0.655 ± 14 μm for finish machined SS316L steel fabricated using LPBF. For CNC milling, the surface roughness lies in the range of 0.2 μm to 25 μm, with more frequent applications reporting a surface roughness between 1.6 μm to 6.3 μm [63]. Hence, it can be concluded that WAAM-fabricated components with appropriate finish machining parameters can demonstrate surface integrity comparable to LPBF and CNC machined parts.

4.5.2 Tensile test

Tensile tests were conducted in accordance with ASTM E8/E8M [51] standard for two WAAM samples each in horizontal and vertical orientation under a displacement rate of 1 mm/min. The results of the tensile test are displayed in Fig. 17. An average ultimate tensile strength of 1002 and 700 MPa are observed in the horizontal and vertical orientations of WAAM samples, respectively. The average yield strength of 694 and 574 MPa are obtained for WAAM samples in the horizontal and vertical orientations, respectively. Likewise, average elongations at break of 19% and 12% are obtained for horizontally and vertically oriented WAAM samples, correspondingly. These mechanical properties of WAAM samples are also compared with those of its parent material, i.e. low carbon steel (carbon content < 0.2%). The average mechanical properties of low carbon steels are taken from the MatWeb database [64]. It is seen that overall WAAM exhibits good mechanical strength and ductility, comparable to its parent material. However, an anisotropy

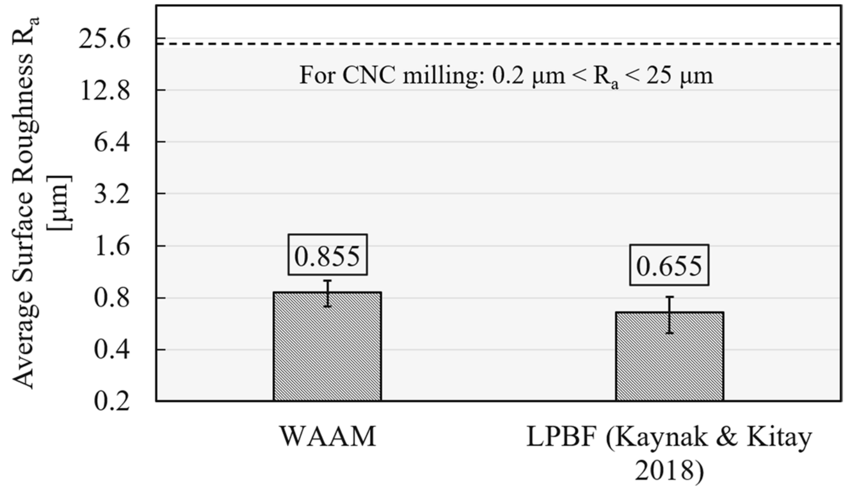

Fig. 16 Average surface roughness values for WAAM, LPBF, and CNC milling

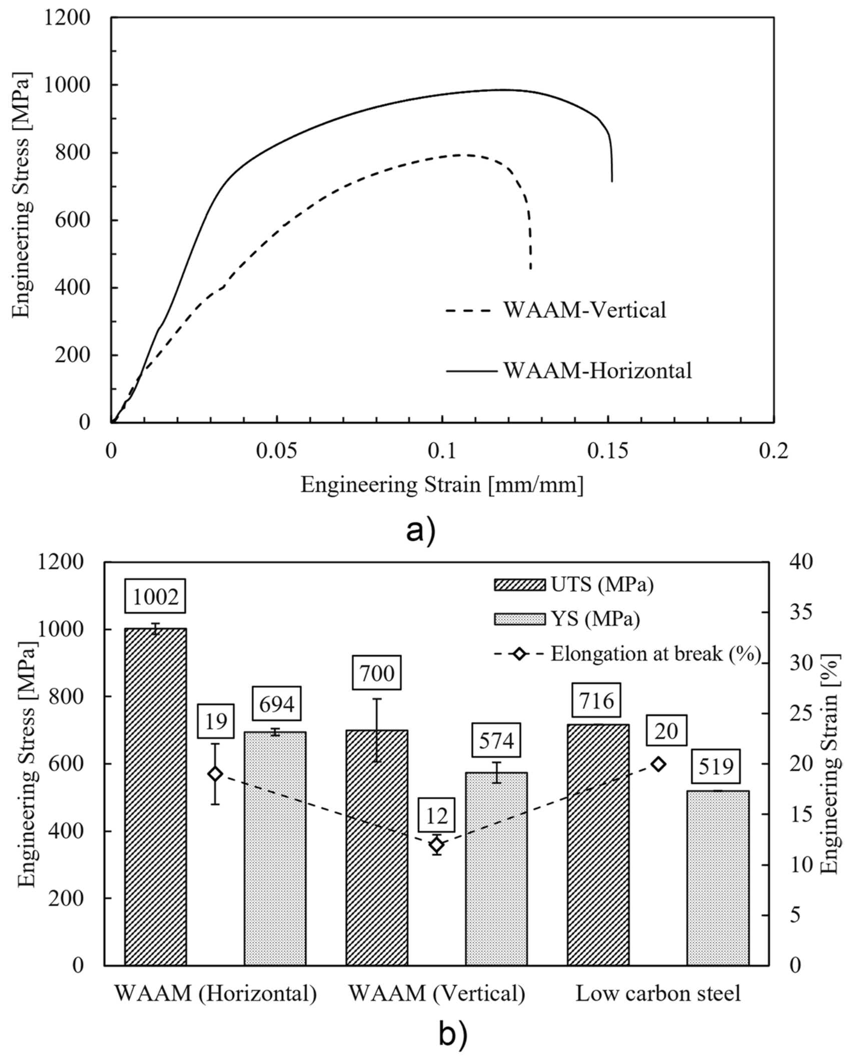

Fig. 17 **a** Stress–strain curve for WAAM specimens. **b** Yield strength (YS), ultimate tensile strength (UTS), and elongation at break comparisons for WAAM specimens and low carbon steel

is observed in its mechanical properties due to its layer-by-layer deposition and anisotropic material grain growth. For the average ultimate tensile strength, WAAM shows a 30% lower value in vertical direction compared to horizontal direction. Similarly, the average yield stress in vertical orientation is 20% lower than that in horizontal one. Likewise, the mean elongation at break for WAAM in vertical direction is about 40% lower than mean elongation at break in horizontal direction. The use of post-process heat treatments could be considered to improve and uniformize the mechanical response of the WAAM-fabricated parts.

Furthermore, the tensile properties obtained by WAAM in this study were also compared with those obtained in previous studies of WAAM [65–69], LPBF [70–72] and CNC machining of steels [73–75] existing in the scientific literature (refer to Fig. 18). The tensile properties obtained in this study lied well within the intervals reported in the scientific literature.

4.5.3 Hardness test

Hardness tests were performed in accordance with ISO 6507–1:2023 standard [52] for WAAM samples in horizontal and vertical directions. The results are depicted in Fig. 19. In the horizontal direction, the hardness varied in the range of 278 to 363 HV with an average of 313 HV. On the other hand, an average hardness of 302 HV, lying between 273 and 332 HV, was reported in the vertical specimen. In both orientations, Vickers hardness values for WAAM specimens were higher than the average value of 266 HV for its parent material, as obtained from [64].

4.5.4 Microstructural characterization

The microstructure of the HSLA steel sample fabricated by WAAM exhibits heterogeneity along the build-up direction (refer to Fig. 20). In WAAM, the top part of the previous layer is remelted during the deposition of a new layer, altering the microstructure at the interface between consecutive layers. The final microstructure of WAAM-fabricated HSLA steels generally exhibit ferrites (acicular and quasi-polygonal), bainite, pearlite, and martensite or martensite-austenite

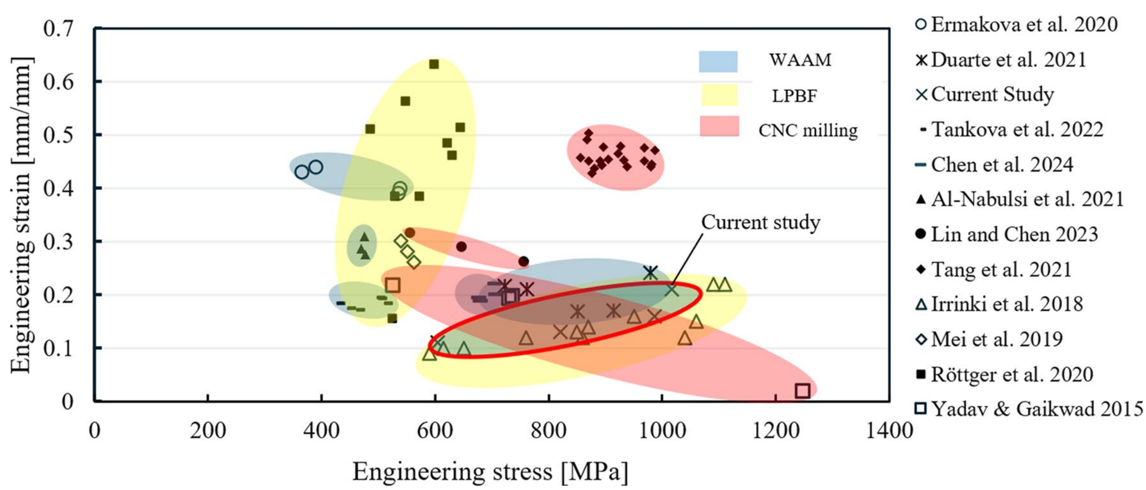

Fig. 18 Comparison of tensile properties of steels manufactured by CNC machining, WAAM, and LPBF

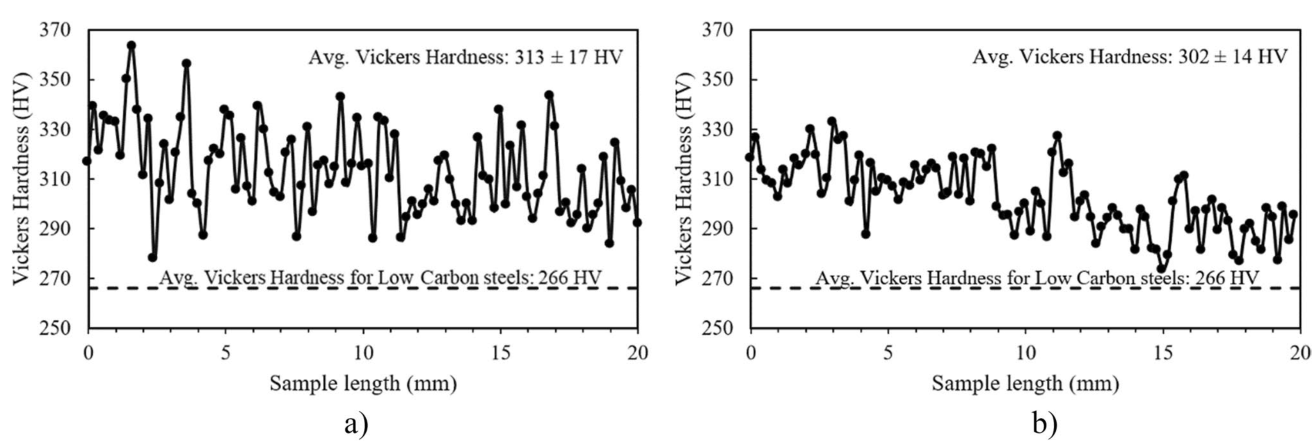

Fig. 19 Hardness variation in WAAM samples for **a** horizontal orientation and **b** vertical orientation

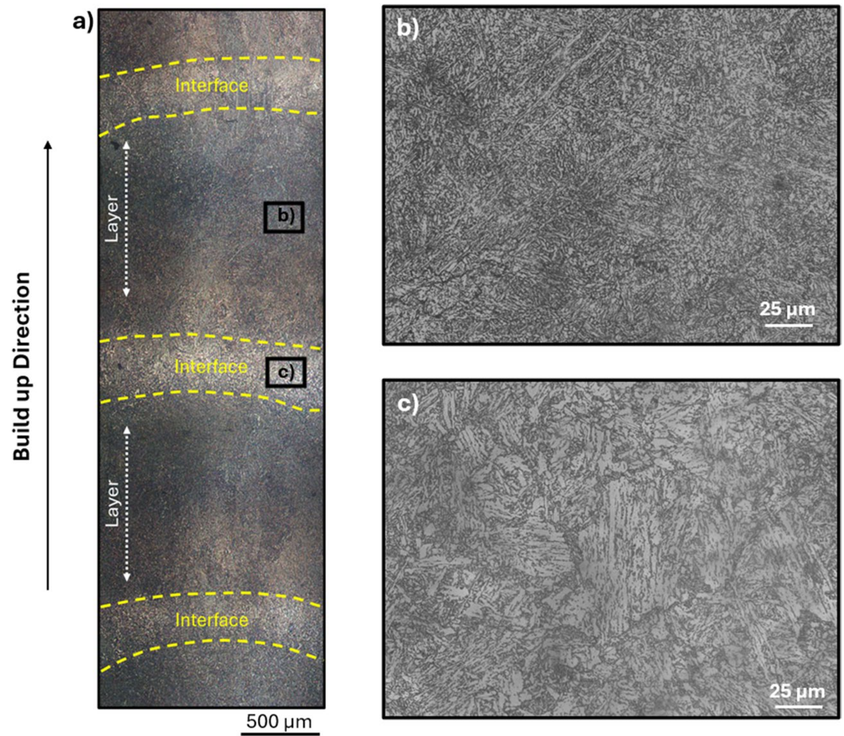

Fig. 20 Microstructure of the WAAM wall: **a** macrograph exhibiting the layers and their interface, **b** detailed view of the microstructure within the layers, revealing a high amount of ferrite (black phase) that martensite-austenite (white phase), **c** detailed view of the microstructure at the interface where higher fraction of martensite-austenite can be observed

phases [76, 77]. In this study, coarser grain sizes with a higher composition of martensite-austenite are observed at interfaces, while finer grain sizes with a higher composition of ferrite are observed within the layers. This microstructural heterogeneity explains the anisotropy in mechanical properties. Samples in vertical orientations exhibit higher microstructural heterogeneity due to the presence of multiple layers and interfaces, resulting in inferior mechanical properties compared to samples in horizontal orientations.

Based on the results of mechanical and microstructural characterizations, it is seen that although WAAM specimens demonstrate mechanical properties comparable to those of its parent material, an anisotropy is seen in their mechanical properties. This is a common occurrence in additively manufactured metal parts reported in various studies [65, 66, 76, 78], where better mechanical properties are seen in the horizontal direction than in the vertical direction. However, as showed by Duarte et al. [66], it possible to improve mechanical properties of WAAM by varying process parameters like wire feed speed, travel speed, deposition rate, and heat input or by post-process heat treatments.

5 Conclusions

In this study, a cradle to gate life cycle assessment and costing of a WAAM manufactured part is carried out and its environmental, economic, and mechanical performance is compared with CNC machining and LPBF approaches. The findings of this study are listed as follows:

- For the mechanical part studied, WAAM demonstrated 40% material reduction and, hence, was seen as the most environmentally benign approach, followed by CNC milling approach. While CNC milling exhibits slightly higher environmental impact than WAAM (by 8%), an environmental impact over 4 times of WAAM is seen for LPBF.
- Raw material is the major environmental hotspot accounting for 51% and 75% of the total environmental impact of WAAM and CNC milling. However, for LPBF, it is the energy consumed during process responsible for 36% of the total environmental impact.
- Labour is the main cost driver in CNC milling approach responsible for 66% of the production cost. For WAAM, the post-processing stage is the major contributor to production cost with a share of 45%, while for LPBF, it is the machine cost with a contribution of 48% of the total production cost.
- Although, CNC machining is seen to be the most cost-effective fabrication method for single unit production, WAAM becomes the cheapest option when produced in batch sizes over 3. A significant reduction in production cost for each approach can be seen when produced in higher batch sizes.
- WAAM is seen to be more environmentally friendly and cost-effective option for producing larger scaled up

versions of the part considered. WAAM when used for fabricating larger parts demonstrates significantly better material efficiency than CNC milling leading to remarkable material, environmental impact, and cost savings, complementing to its ability to build large parts.
- WAAM-fabricated part demonstrated good mechanical strength and hardness comparable to its parent material. However, anisotropy in mechanical properties is seen with better mechanical properties in orientation along the build direction (horizontal direction).

The scope of the current study is limited to the production phase of components. As WAAM becomes more mature, the scope should be extended to operational, repair and maintenance, and disposal phases of WAAM parts when more data for these phases becomes available. The current study investigated a small (< 200 g) and moderately complex geometry in order to collect experimental data for building LCA and LCC scenarios. Nevertheless, the experimental data presented in this study can be utilized for LCA and LCC assessments of other WAAM product geometries. Future studies will analyse highly complex industrial products with real-life applications based on inventories collected in this study. Based on the experimental data recorded in this study, predictive environmental impact and cost models for WAAM products will also be developed in future that will help manufacturers in quick and cost-effective decision-making on choice of the most sustainable process for their products. Additionally, the social impacts of WAAM on its different stakeholders' needs be assessed using social-life cycle assessment methodology for a comprehensive understanding of its environmental, economic, and social dimensions of sustainability. From a technological perspective, future research should explore the potential of WAAM for manufacturing complex geometries and developing novel materials to expand its applications. Additionally, efforts should focus on improving the dimensional accuracy, surface finish, and mechanical properties of WAAM components by optimizing parameters, developing innovative post-processing methods, and enhancing monitoring and control systems.

Appendix

Table 7 Environmental impacts of WAAM, CNC milling, and LPBF

Impact category	Unit	WAAM	CNC milling	LPBF
Global warming	kg CO2 eq	2.00E + 00	1.65E + 00	1.15E + 01
Stratospheric ozone depletion	kg CFC11 eq	6.71E − 07	4.63E − 07	4.69E − 06
Ionizing radiation	kBq Co-60 eq	3.33E − 01	8.87E − 02	3.22E + 00
Ozone formation, human health	kg NOx eq	4.46E − 03	4.10E − 03	2.53E − 02
Fine particulate matter formation	kg PM2.5 eq	3.16E − 03	2.81E − 03	1.83E − 02
Ozone formation, terrestrial ecosystems	kg NOx eq	4.62E − 03	4.30E − 03	2.56E − 02
Terrestrial acidification	kg SO2 eq	7.33E − 03	5.95E − 03	4.92E − 02
Freshwater eutrophication	kg P eq	1.13E − 03	7.39E − 04	7.80E − 03
Marine eutrophication	kg N eq	8.62E − 05	5.22E − 05	5.47E − 04
Terrestrial ecotoxicity	kg 1,4-DCB	5.50E + 00	6.48E + 00	1.18E + 01
Freshwater ecotoxicity	kg 1,4-DCB	1.08E − 01	1.07E − 01	4.45E − 01
Marine ecotoxicity	kg 1,4-DCB	1.47E − 01	1.47E − 01	5.92E − 01
Human carcinogenic toxicity	kg 1,4-DCB	7.36E − 01	8.57E − 01	1.20E + 00
Human non-carcinogenic toxicity	kg 1,4-DCB	2.01E + 00	1.59E + 00	1.15E + 01
Land use	m2a crop eq	4.89E − 02	4.05E − 02	2.55E − 01
Mineral resource scarcity	kg Cu eq	4.70E − 02	6.46E − 02	5.47E − 02
Fossil resource scarcity	kg oil eq	5.00E − 01	4.08E − 01	3.14E + 00
Water consumption	m3	4.09E − 02	1.38E − 02	3.23E − 01

Acknowledgements Samruddha Kokare acknowledges Fundação para a Ciência e a Tecnologia (FCT–MCTES) for its financial support via the MIT-Portugal Program PhD grant PRT/BD/154651/2023. Jiajia Shen acknowledges the China Scholarship Council for funding the Ph.D. grant CSC No. 201808320394. Pedro Fonseca acknowledges FCT–MCTES for funding the PhD grant 2022.13883.BD. J.G. Lopes acknowledges FCT–MCTES for its financial support via the Ph.D. grant 2020.07350.BD. J. P. Oliveira acknowledges funding by national funds from FCT–Fundação para a Ciência e a Tecnologia, I.P., in the scope of the projects LA/P/0037/2020, UIDP/50025/2020, and UIDB/50025/2020 of the Associate Laboratory Institute of Nanostructures, Nanomodelling and Nanofabrication–i3N. Samruddha Kokare, Radu Godina, Telmo G. Santos, and Carla M. Machado acknowledge Fundação para a Ciência e a Tecnologia (FCT–MCTES) for its financial support for its financial support via the project UIDP/00667/2020 and UIDB/00667/2020 (UNIDEMI). This activity has received funding from the European Institute of Innovation and Technology (EIT)–Project Smart WAAM: Microstructural Engineering and Integrated Non-Destructive Testing. This body of the European Union receives support from the European Union's Horizon 2020 research and innovation programme.

Author contribution Samruddha Kokare: writing—original draft, experimentation, investigation, formal analysis, data curation. Jiajia Shen: investigation, formal analysis, data curation. Pedro Fonseca: experimentation and data curation. J.G. Lopes: experimentation and data curation; writing—review and editing. Carla M. Machado: experimentation and data curation. Telmo G. Santos: writing—review and editing, validation, supervision, methodology, conceptualization. J.P. Oliveira: writing—review and editing; validation; supervision; resources; conceptualization. Radu Godina: writing—review and editing; validation; supervision; conceptualization.

Funding Open access funding provided by FCT|FCCN (b-on). Samruddha Kokare acknowledges Fundação para a Ciência e a Tecnologia (Portugal) for its financial support via the MIT-Portugal Program PhD grant PRT/BD/154651/2023. Jiajia Shen acknowledges the China Scholarship Council for funding the Ph.D. grant CSC No. 201808320394. Pedro Fonseca acknowledges FCT–MCTES for funding the PhD grant 2022.13883.BD. J.G. Lopes acknowledges FCT–MCTES for its financial support via the Ph.D. grant 2020.07350.BD. J. P. Oliveira acknowledges funding by national funds from FCT–Fundação para a Ciência e a Tecnologia, I.P., in the scope of the projects LA/P/0037/2020, UIDP/50025/2020, and UIDB/50025/2020 of the Associate Laboratory Institute of Nanostructures, Nanomodelling and Nanofabrication–i3N. Samruddha Kokare, Radu Godina, Telmo G. Santos, and Carla M. Machado acknowledge Fundação para a Ciência e a Tecnologia (FCT-MCTES) for its financial support for its financial support via the project UIDP/00667/2020 and UIDB/00667/2020 (UNIDEMI). This activity has received funding from the European Institute of Innovation and Technology (EIT)–Project Smart WAAM: Microstructural Engineering and Integrated Non-Destructive Testing. This body of the European Union receives support from the European Union's Horizon 2020 research and innovation programme.

Data availability Data will be made available on request.

Code availability Not applicable.

Declarations

Ethics approval Not applicable.

Consent to participate Not applicable.

Consent for publication Not applicable.

Conflicts of interest The authors declare no competing interests.

References

1. IEA, "Share of electricity final consumption by sector, 2019, IEA, Paris, Licence: CC BY 4.0." 2021. [Online]. Available: https://www.iea.org/data-and-statistics/charts/share-of-electricity-final-consumption-by-sector-2019. Accessed 06 Jun 2024
2. Worrell E, Allwood J, Gutowski T (2016) The role of material efficiency in environmental stewardship. Annu Rev Environ Resour 41(1):575–598. https://doi.org/10.1146/annurev-environ-110615-085737
3. United Nations Framework Convention on Climate Change (UNFCCC), "Kyoto Protocol to the United Nations Framework Convention on Climate Change." Dec. 10, 1997. [Online]. Available: https://unfccc.int/documents/2409. Accessed 04 Dec 2023
4. UNFCCC. Conference of the Parties (COP), "Report of the Conference of the Parties on its twenty-first session, held in Paris from 30 November to 13 December 2015." Jul. 29, 2016. [Online]. Available: https://unfccc.int/documents/9096. Accessed 04 Dec 2023
5. European Council, "European Green Deal". [Online]. Available: https://www.consilium.europa.eu/en/policies/green-deal/. Accessed 04 Dec 2023
6. Despeisse M, Mbaye F, Ball PD, Levers A (2012) The emergence of sustainable manufacturing practices. Prod Plan Control 23(5):354–376. https://doi.org/10.1080/09537287.2011.555425
7. Mitchell GR (2017) Climate change and manufacturing. Procedia Manuf 12:298–306. https://doi.org/10.1016/j.promfg.2017.08.033
8. Sprengel DC, Busch T (2011) Stakeholder engagement and environmental strategy – the case of climate change. Bus Strat Env 20(6):351–364. https://doi.org/10.1002/bse.684
9. Wang D (2017) A comparative study of firm-level climate change mitigation targets in the European Union and the United States. Sustainability 9(4):489. https://doi.org/10.3390/su9040489
10. Machado CG, Winroth MP, Ribeiro Da Silva EHD (2020) Sustainable manufacturing in Industry 4.0: an emerging research agenda. Int J Prod Res 58(5):1462–1484. https://doi.org/10.1080/00207543.2019.1652777
11. Garetti M, Taisch M (2012) Sustainable manufacturing: trends and research challenges. Prod Plan Control 23(2–3):83–104. https://doi.org/10.1080/09537287.2011.591619
12 Abdul Rashid SH, Evans S, Longhurst P (2008) A comparison of four sustainable manufacturing strategies. Int J Sustain Eng 1(3):214–229. https://doi.org/10.1080/19397030802513836
13. Van Caneghem J, Block C, Cramm P, Mortier R, Vandecasteele C (2010) Improving eco-efficiency in the steel industry: the

ArcelorMittal Gent case. J Clean Prod 18(8):807–814. https://doi.org/10.1016/j.jclepro.2009.12.016
14. Allwood JM, Ashby MF, Gutowski TG, Worrell E (2011) Material efficiency: a white paper. Resour Conserv Recycl 55(3):362–381. https://doi.org/10.1016/j.resconrec.2010.11.002
15. ISO/ASTM 52900 (2021) Standard terminology for additive manufacturing-general principles-fundamentals and vocabulary. [Online]. Available: https://www.iso.org/standard/74514.html. Accessed 06 Jun 2024
16. Xia C et al (2020) Model predictive control of layer width in wire arc additive manufacturing. J Manuf Process 58:179–186. https://doi.org/10.1016/j.jmapro.2020.07.060
17. Lunetto V, Priarone PC, Kara S, Settineri L (2021) A comparative LCA method for environmentally friendly manufacturing: additive manufacturing versus machining case. Procedia CIRP pp 406–411. https://doi.org/10.1016/j.procir.2021.01.125
18. Ngo TD, Kashani A, Imbalzano G, Nguyen KTQ, Hui D (2018) Additive manufacturing (3D printing): a review of materials, methods, applications and challenges. Compos B Eng 143:172–196. https://doi.org/10.1016/j.compositesb.2018.02.012
19. Tseng M-L, Aslam MI, Ismail EAA, Awwad FA, Gorji NE (2024) CT scan, EBSD and nanoindentation analysis of 3D-printed parts with post-process heat-treatment. Metall Res Technol 121(1):101. https://doi.org/10.1051/metal/2023083
20. Liu J, Xu Y, Ge Y, Hou Z, Chen S (2020) Wire and arc additive manufacturing of metal components: a review of recent research developments. Int J Adv Manuf Technol 111(1–2):149–198. https://doi.org/10.1007/s00170-020-05966-8
21. Taşdemir A, Nohut S (2021) An overview of wire arc additive manufacturing (WAAM) in shipbuilding industry. Ships Offshore Struct 16(7):797–814. https://doi.org/10.1080/17445302.2020.1786232
22. Williams SW, Martina F, Addison AC, Ding J, Pardal G, Colegrove P (2016) Wire + Arc Additive Manufacturing. Mater Sci Technol 32(7):641–647. https://doi.org/10.1179/1743284715Y.0000000073
23. Jafari D, Vaneker THJ, Gibson I (2021) Wire and arc additive manufacturing: Opportunities and challenges to control the quality and accuracy of manufactured parts. Mater Des 202:109471. https://doi.org/10.1016/j.matdes.2021.109471
24. Ding D, Pan Z, Cuiuri D, Li H (2015) Wire-feed additive manufacturing of metal components: technologies, developments and future interests. Int J Adv Manuf Technol 81(1–4):465–481. https://doi.org/10.1007/s00170-015-7077-3
25. Laleh M et al (2023) Heat treatment for metal additive manufacturing. Prog Mater Sci 133:101051. https://doi.org/10.1016/j.pmatsci.2022.101051
26. Shah A, Aliyev R, Zeidler H, Krinke S (2023) A review of the recent developments and challenges in wire arc additive manufacturing (WAAM) process. JMMP 7(3):97. https://doi.org/10.3390/jmmp7030097
27. Nagamatsu H, Sasahara H, Mitsutake Y, Hamamoto T (2020) Development of a cooperative system for wire and arc additive manufacturing and machining. Addit Manuf 31:100896. https://doi.org/10.1016/j.addma.2019.100896
28. Kokare S, Oliveira JP, Godina R (2023) Life cycle assessment of additive manufacturing processes: a review. J Manuf Syst 68:536–559. https://doi.org/10.1016/j.jmsy.2023.05.007
29. Böckin D, Tillman A-M (2019) Environmental assessment of additive manufacturing in the automotive industry. J Clean Prod 226:977–987. https://doi.org/10.1016/j.jclepro.2019.04.086
30. Kamps T, Lutter-Guenther M, Seidel C, Gutowski T, Reinhart G (2018) Cost- and energy-efficient manufacture of gears by laser beam melting. CIRP J Manuf Sci Technol 21:47–60. https://doi.org/10.1016/j.cirpj.2018.01.002
31. Huang R et al (2016) Energy and emissions saving potential of additive manufacturing: the case of lightweight aircraft components. J Clean Prod 135:1559–1570. https://doi.org/10.1016/j.jclepro.2015.04.109
32. Torres-Carrillo S, Siller HR, Vila C, López C, Rodríguez CA (2020) Environmental analysis of selective laser melting in the manufacturing of aeronautical turbine blades. J Clean Prod 246. https://doi.org/10.1016/j.jclepro.2019.119068
33. Paris H, Mokhtarian H, Coatanéa E, Museau M, Ituarte IF (2016) Comparative environmental impacts of additive and subtractive manufacturing technologies. CIRP Ann Manuf Technol 65(1):29–32. https://doi.org/10.1016/j.cirp.2016.04.036
34. Peng T, Wang Y, Zhu Y, Yang Y, Yang Y, Tang R (2020) Life cycle assessment of selective-laser-melting-produced hydraulic valve body with integrated design and manufacturing optimization: a cradle-to-gate study. Addit Manuf 36. https://doi.org/10.1016/j.addma.2020.101530
35. Guarino S, Ponticelli GS, Venettacci S (2020) Environmental assessment of Selective Laser Melting compared with Laser Cutting of 316L stainless steel: a case study for flat washers' production. CIRP J Manuf Sci Technol 31:525–538. https://doi.org/10.1016/j.cirpj.2020.08.004
36. Cappucci GM, Pini M, Neri P, Marassi M, Bassoli E, Ferrari AM (2020) Environmental sustainability of orthopedic devices produced with powder bed fusion. J Ind Ecol 24(3):681–694. https://doi.org/10.1111/jiec.12968
37. Lyons R, Newell A, Ghadimi P, Papakostas N (2021) Environmental impacts of conventional and additive manufacturing for the production of Ti-6Al-4V knee implant: a life cycle approach. Int J Adv Manuf Technol 112(3–4):787–801. https://doi.org/10.1007/s00170-020-06367-7
38. Priarone PC, Pagone E, Martina F, Catalano AR, Settineri L (2020) Multi-criteria environmental and economic impact assessment of wire arc additive manufacturing. CIRP Ann 69(1):37–40. https://doi.org/10.1016/j.cirp.2020.04.010
39. Bekker ACM, Verlinden JC (2018) Life cycle assessment of wire + arc additive manufacturing compared to green sand casting and CNC milling in stainless steel. J Clean Prod 177:438–447. https://doi.org/10.1016/j.jclepro.2017.12.148
40. Shah IH, Hadjipantelis N, Walter L, Myers RJ, Gardner L (2023) Environmental life cycle assessment of wire arc additively manufactured steel structural components. J Clean Prod 389:136071. https://doi.org/10.1016/j.jclepro.2023.136071
41. Kokare S, Oliveira JP, Santos TG, Godina R (2023) Environmental and economic assessment of a steel wall fabricated by wire-based directed energy deposition. Addit Manuf 61:103316. https://doi.org/10.1016/j.addma.2022.103316
42. Kokare S, Oliveira JP, Godina R (2023) A LCA and LCC analysis of pure subtractive manufacturing, wire arc additive manufacturing, and selective laser melting approaches. J Manuf Process 101:67–85. https://doi.org/10.1016/j.jmapro.2023.05.102
43. Pusateri V, Olsen SI, Hauschild MZ, Kara S (2023) Potential for absolute sustainability of wire-arc additive manufacturing: a boat propellers case. CIRP Ann 72(1):29–32. https://doi.org/10.1016/j.cirp.2023.04.034
44. Peng S et al (2017) Toward a sustainable impeller production: environmental impact comparison of different impeller manufacturing methods. J Ind Ecol 21:S216–S229. https://doi.org/10.1111/jiec.12628
45. ISO 14044 (2006) Environmental management—life cycle assessment—requirements and guidelines. [Online]. Available: https://www.iso.org/standard/38498.html. Accessed 06 Jun 2024
46. IEC 60300-3-3 (2017) Dependability management–Part 3-3: Application guide–Life cycle costing. Available: https://webstore.iec.ch/en/publication/31206. Accessed 06 Jun 2024

47. ISO 15686–5 (2017) Buildings and constructed assets. service life planning. life-cycle costing. [Online]. Available: https://www.iso.org/standard/61148.html. Accessed 06 Jun 2024
48. Dhillon BS (2017) Life cycle costing for engineers. First issued in paperback. New York: CRC Press, Boca Raton, London
49. Greene LE, Shaw BL (1990) The steps for successful life cycle cost analysis. In: IEEE Conference on Aerospace and Electronics, Dayton, OH, USA: IEEE, pp 1209–1216. https://doi.org/10.1109/NAECON.1990.112942
50. TWI Ltd., "What is mechanical testing? (a complete guide)." [Online]. Available: https://www.twi-global.com/technical-knowledge/faqs/what-is-mechanical-testing#Advantages. Accessed 04 Dec 2023
51. ASTM E8/E8M-22 (2022) Standard test methods for tension testing of metallic materials. [Online]. Available:https://www.astm.org/e0008_e0008m-22.html. Accessed 06 Jun 2024
52. ISO 6507-1 (2023) Metallic materials vickers hardness test Part 1: Test method. [Online]. Available:https://www.iso.org/standard/83898.html. Accessed 06 Jun 2024
53. Ecoinvent, "Ecoinvent 3 Database". [Online]. Available: https://ecoinvent.org/the-ecoinvent-database/. Accessed 27 Feb 2023
54. Hassanin H, Elshaer A, Benhadj-Djilali R, Modica F, Fassi I (2018) Surface finish improvement of additive manufactured metal parts. In: Gupta K (ed) Micro and Precision Manufacturing, in Engineering Materials, Cham: Springer International Publishing, pp 145–164. https://doi.org/10.1007/978-3-319-68801-5_7
55. Ingarao G, Priarone PC, Deng Y, Paraskevas D (2018) Environmental modelling of aluminium based components manufacturing routes: Additive manufacturing versus machining versus forming. J Clean Prod 176:261–275. https://doi.org/10.1016/j.jclepro.2017.12.115
56. Gebbe C, Lutter-Günther M, Greiff B, Glasschröder J, Reinhart G (2015) Measurement of the resource consumption of a selective laser melting process. AMM 805:205–212. https://doi.org/10.4028/www.scientific.net/AMM.805.205
57. Eurostat, "Electricity price statistics". [Online]. Available: https://ec.europa.eu/eurostat/statistics-explained/index.php?title=Electricity_price_statistics. Accessed 20 Dec 2021
58. Statistica, "Average hourly labor cost in selected European countries in 2020". [Online]. Available: https://www.statista.com/statistics/1211601/hourly-labor-cost-in-europe/. Accessed 20 Dec 2021
59. Priarone PC, Campatelli G, Catalano AR, Baffa F (2021) Life-cycle energy and carbon saving potential of wire arc additive manufacturing for the repair of mold inserts. CIRP J Manuf Sci Technol 35:943–958. https://doi.org/10.1016/j.cirpj.2021.10.007
60. Pagone E, Antonissen J, Martina F (2022) Life cycle sustainability assessment of repair through wire and arc additive manufacturing. In: Minerals, Metals and Materials Series, pp 387–394. https://doi.org/10.1007/978-3-030-92563-5_39
61. ISO 21920–2 (2021) Geometrical product specifications (GPS)—Surface texture: Profile—Part 2: Terms, definitions and surface texture parameters
62. Kaynak Y, Kitay O (2018) Porosity, Surface Quality, Microhardness and microstructure of selective laser melted 316L stainless steel resulting from finish machining. JMMP 2(2):36. https://doi.org/10.3390/jmmp2020036
63. Grzesik W, Kruszynski B, Ruszaj A (2010) Surface integrity of machined surfaces. In: Davim JP (ed) Surface Integrity in Machining, London: Springer London, pp 143–179. https://doi.org/10.1007/978-1-84882-874-2_5
64. MatWeb Database, Material property data. [Online]. Available: https://www.matweb.com/index.aspx. Accessed 09 Nov 2023
65. Ermakova A, Mehmanparast A, Ganguly S, Razavi N, Berto F (2020) Investigation of mechanical and fracture properties of wire and arc additively manufactured low carbon steel components. Theoret Appl Fract Mech 109:102685. https://doi.org/10.1016/j.tafmec.2020.102685
66. Duarte VR, Rodrigues TA, Schell N, Santos TG, Oliveira JP, Miranda RM (2021) Wire and arc additive manufacturing of high-strength low-alloy steel: microstructure and mechanical properties. Adv Eng Mater 23(11):2001036. https://doi.org/10.1002/adem.202001036
67. Tankova T, Andrade D, Branco R, Zhu C, Rodrigues D, Simões Da Silva L (2022) Characterization of robotized CMT-WAAM carbon steel. J Constr Steel Res 199:107624. https://doi.org/10.1016/j.jcsr.2022.107624
68. Chen M-T et al (2024) Mechanical properties and microstructure characteristics of wire arc additively manufactured high-strength steels. Eng Struct 300:117092. https://doi.org/10.1016/j.engstruct.2023.117092
69. Al-Nabulsi Z, Mottram JT, Gillie M, Kourra N, Williams MA (2021) Mechanical and X ray computed tomography characterisation of a WAAM 3D printed steel plate for structural engineering applications. Constr Build Mater 274:121700. https://doi.org/10.1016/j.conbuildmat.2020.121700
70. Irrinki H et al (2018) Effects of particle characteristics on the microstructure and mechanical properties of 17–4 PH stainless steel fabricated by laser-powder bed fusion. Powder Technol 331:192–203. https://doi.org/10.1016/j.powtec.2018.03.025
71. Mei X, Wang X, Peng Y, Gu H, Zhong G, Yang S (2019) Interfacial characterization and mechanical properties of 316L stainless steel/inconel 718 manufactured by selective laser melting. Mater Sci Eng, A 758:185–191. https://doi.org/10.1016/j.msea.2019.05.011
72. Röttger A et al (2020) Microstructure and mechanical properties of 316L austenitic stainless steel processed by different SLM devices. Int J Adv Manuf Technol 108(3):769–783. https://doi.org/10.1007/s00170-020-05371-1
73. Yadav D, Gaikwad A (2015) Comparison and testing of tensile strength for low & medium carbon steel. Int J Mech Eng (IJME) 4(5):1–8
74. Li W, Chen H (2023) Tensile performance of normal and high-strength structural steels at high strain rates. Thin-Walled Struct 184:110457. https://doi.org/10.1016/j.tws.2022.110457
75. Tang J, He M, Qiao Y, Xia M, Tao Z (2021) Tensile behavior of a novel high-strength and high-toughness steel at strain rates from 0.1 s−1 to 1000 s−1. Constr Build Mater 304:124606. https://doi.org/10.1016/j.conbuildmat.2021.124606
76. Rodrigues TA, Duarte V, Avila JA, Santos TG, Miranda RM, Oliveira JP (2019) Wire and arc additive manufacturing of HSLA steel: Effect of thermal cycles on microstructure and mechanical properties. Addit Manuf 27:440–450. https://doi.org/10.1016/j.addma.2019.03.029
77. Song K et al (2023) Microstructure and mechanical properties of high-strength, low-alloy steel thin-wall fabricated with wire and arc additive manufacturing. Metals 13(4):764. https://doi.org/10.3390/met13040764
78. Kok Y et al (2018) Anisotropy and heterogeneity of microstructure and mechanical properties in metal additive manufacturing: a critical review. Mater Des 139:565–586. https://doi.org/10.1016/j.matdes.2017.11.021